united nations
educational, scientific
and cultural
organization

international atomic
energy agency

the
abdus salam
international centre for theoretical physics

Winter College on Optics and Photonics
7 - 25 February 2000

1218-11

"Laser Beam Characterization"

M. SANTARSIERO
Università Roma Tre
Dipt. Fisica
Italy

Laser Beam Characterization

Massimo Santarsiero

Dip. di Fisica, Università Roma Tre

Roma (Italy)

ICTP/ICO/OSA Winter College on Optics and Photonics

Miramare - Trieste, Italy, 7-25 February 2000

Contents

1 PRELIMINARIES

In the present Chapter, we report some of the main results to be used in the study of the propagation of light beams. In particular, we recall the paraxial wave equation and give the expression of the (fundamental and higher-order) Gaussian beams.

1.1 The paraxial wave equation

We consider only quasi-monochromatic light beams and we suppose that all we have to know about the radiation properties can be derived from one scalar quantity, say U, which is the analytical signal associated to a general component of the electromagnetic field carried by the radiation. Under these hypotheses, the general solution of a propagation problem in vacuo can be obtained by solving the following Helmholtz equation:

$$\nabla^2 U(\mathbf{r}, z) + k^2 U(\mathbf{r}, z) = 0 \,, \tag{1}$$

where $\mathbf{r}$ and z are the transversal and longitudinal coordinates, respectively, of a suitable reference frame, and $k = 2\pi/\lambda$ is the wavenumber.

It is customary to write the function $U(\mathbf{r}, z)$ in the following form:

$$U(\mathbf{r}, z) = \psi(\mathbf{r}, z) \exp(ikz) \,, \tag{2}$$

which is particularly fit to introduce the paraxial approximation. In fact, when the function $\psi(\mathbf{r}, z)$ is sufficiently smooth with respect to z, if compared to the oscillating term $\exp(ikz)$, then Eq. (1) can be replaced by [1]

$$\nabla_\perp^2 \psi(\mathbf{r}, z) + 2ik\partial_z \psi(\mathbf{r}, z) = 0 \,, \tag{3}$$

which is the paraxial wave equation. Here, the symbol $\nabla_\perp^2$ denotes the Laplacian operator wth respect to the coordinates across the transverse plane.

It is well known that Eq. (3) holds, in particular, in those cases when the light distribution, during propagation, remains almost concentrated around the z-axis and then it can be used in the study of the propagation of light beams.

It can be easily shown that one solution of Eq. (3) is

$$\psi(\mathbf{r}, z) = \frac{1}{q(z)} \exp\left[\frac{ikr^2}{2q(z)}\right] \,, \tag{4}$$

where the function $q(z)$ must satisfy the following condition:

$$q'(z) = 1 \ . \tag{5}$$

To this aim, a possible function is $q(z) = z - z_0$, which leads to a solution of the form

$$\psi(\mathbf{r}, z) = \frac{1}{z - z_0} \exp\left[\frac{ikr^2}{2(z - z_0)}\right] \ , \tag{6}$$

which coincides with a spherical wave centered on the $z-$axis at $z = z_0$. When the paraxial conditions are met, indeed, a spherical wave can be approximated as

$$\frac{1}{z - z_0} \exp\left[ik\sqrt{r^2 + (z - z_0)^2}\right] \approx \frac{1}{z - z_0} \exp\left\{ik\left[(z - z_0) + \frac{r^2}{2(z - z_0)}\right]\right\} \ , \tag{7}$$

which is exactly of the form (6).

Equation (6) establishes the link between the paraxial wave equation and the Fresnel propagation formula [2]

$$\psi(\mathbf{r}, z) = \frac{-i}{\lambda z} \int U(\vec{\rho}, 0) \exp\left[i\frac{\pi}{\lambda z}(\vec{\rho} - \mathbf{r})^2\right] \mathrm{d}^2\vec{\rho} \ , \tag{8}$$

where the solution is expressed as a linear combination of functions of the form (6) with $z_0 = 0$ and therefore is still a solution of the paraxial wave equation.

A slightly more general expression of $q(z)$ satisfying condition (5) gives rise to the Gaussian beams as will be shown in the next Section.

1.2 The fundamental Gaussian beam

A different functional form satisfying condition (5) is the following:

$$q(z) = z - z_0 - iL \ . \tag{9}$$

with L a positive parameter.

On introducing the latter expression into the solution of the paraxial wave equation [Eq. (4)], one obtains

$$\psi(\mathbf{r},z)=\frac{w(z_0)}{w(z)}\exp\left[-i\Phi(z)\right]\exp\left\{\left[\frac{ik}{2R(z)}-\frac{1}{w^2(z)}\right]r^2\right\}\ , \tag{10}$$

where the following parameters have been introduced:

$$w(z)=w(z_0)\sqrt{1+\left(\frac{z-z_0}{L}\right)^2}\ . \tag{11}$$

$$R(z)=(z-z_0)\left[1+\left(\frac{L}{z-z_0}\right)^2\right]\ . \tag{12}$$

$$\Phi(z)=\arctan\left(\frac{z-z_0}{L}\right)\ . \tag{13}$$

and L, which is referred to as the *Rayleigh range* of the beam, is expressed by

$$L=\frac{\pi w^2(z_0)}{\lambda}\ . \tag{14}$$

Parameters in Eqs. (11)-(13) are the spot size, the curvature radius, and the phase anomaly, respectively, of the beam. The axial position $z=z_0$ is referred to as the waist of the beam and coincides with the position where the spot size is minimum, the curvature radius is infinite, and the phase anomaly is zero.

The parameter $q(z)$, introduced in Eq. (9) is referred to as the *complex* radius of curvature of the beam [3] and allows the propagation through paraxial optical systems to be treated in a very simple way, as we shall see. It is related to the real parameters of the Gaussian beam by the relation

$$\frac{1}{q(z)}=\frac{1}{(z-z_0)-iL}=\frac{1}{R(z)}+i\frac{2}{kw^2(z)}\ . \tag{15}$$

When a general optical system can be characterized by a ABCD matrix [4], indeed, the complex radius of curvature of the propagated Gaussian beam, say q_1, is related to the analogous quantity for the input beam, q_0, through the rule [3]

$$q_1=\frac{Aq_0+B}{Cq_0+D}\ , \tag{16}$$

from which the parameters of the propagated beam can be immediately evaluated.

Note that apart from λ the beam is completely characterized by two parameters, namely, position and width of the waist. Furthermore, the chosen reference frame ensures that the beam is centered around the transverse coordinate $\mathbf{r} = 0$ and propagates along the z-axis. In the study of general light beams, of course, transverse location and propagation direction of the beam are to be considered as further free parameters.

In the following, we will refer to the intensity of the field as the square modulus of the function $\psi(\mathbf{r}, z)$. In the case of a Gaussian beam we have

$$I(\mathbf{r}, z) = \frac{w^2(z_0)}{w^2(z)} \exp\left[-\frac{2r^2}{w^2(z)}\right] , \tag{17}$$

so that the transverse intensity is Gaussian at any plane $z = \text{const}$. Furthermore, the total power carried by the beam, conventionally defined as

$$P_{\text{tot}} = \int_{\infty} I(\mathbf{r}, z)\, \mathrm{d}^2 r , \tag{18}$$

turns out to be $\pi w^2(z_0)/2$.

1.3 Higher-order Gaussian beams

Further solutions of the paraxial wave equation are the so-called higher-order Gaussian beams. Depending on the used geometry, we can define two classes of higher-order Gaussian beams: Hermite–Gaussian (HG) beams for rectangular geometry and Laguerre–Gauss (LG) beams for polar geometry [3].

In the first case, we have

$$\begin{aligned} \mathrm{HG}_{\mathrm{nm}}(\mathbf{r}, z) = \; & A \frac{w(z_0)}{w(z)} \exp\left[-i(n+m+1)\Phi(z)\right] \exp\left\{\left[\frac{ik}{2R(z)} - \frac{1}{w^2(z)}\right]\left(x^2+y^2\right)\right\} \\ & \times H_n\left[\frac{\sqrt{2}x}{w(z)}\right] H_m\left[\frac{\sqrt{2}y}{w(z)}\right] . \\ & (n, m = 0, \pm 1, \ldots) \end{aligned} \tag{19}$$

where H_n is the Hermite polynomial [5] of order n and A is an arbitrary constant.

In the case of polar coordinates, we have

$$\mathrm{LG}_{ls}(\mathbf{r},z) = A\frac{w(z_0)}{w(z)}\exp\left[-i(2l+|s|+1)\Phi(z)\right]\exp\left\{\left[\frac{ik}{2R(z)}-\frac{1}{w^2(z)}\right]r^2\right\}$$

$$\times\left[\frac{\sqrt{2}\,r}{w(z)}\right]^{|s|}L_l^{|s|}\left[\frac{2r^2}{w^2(z)}\right]\exp(is\vartheta)\,,$$

$$(l=0,1,\ldots;s=0,\pm1,\ldots) \tag{20}$$

where L_l^s is the Laguerre polynomial [5] of order l and index s. In both cases, the parameters w, R, and Φ are the same as for a Gaussian beam. It is clear that the Gaussian beam presented in the previous section represents the zero-order, or fundamental, member of both the above classes.

A remarkable property of higher-order Gaussian beams is that the shape of their tranverse intensity distribution remains unchanged upon propagation, so that they constitute two classes (actually, the only ones) of *shape-invariant* coherent light beams.

2 PARAMETERS OF A LIGHT BEAM

We saw that Gaussian beams, whose expressions were given in the previous Chapter, are completely specified by a very small number of parameters. Nonetheless, they represent a useful model for many light beams produced by stable laser cavities.

As could be expected, however, one often is faced with cases in which the beam to be analyzed differs significantly from an ideal Gaussian beam, sometimes because of precise requirements about the beam properties. In a general case, it is also rather difficult to find beams parameters that are defined in an unambiguous way and, at the same time, are sufficiently significant for the propagation properties of the beam. This remains true even in the case of continuous-wave, perfectly coherent and uniformly polarized beams, because the significant parameters can be different, depending on the applications one is interested in. For example, one would like to know the total power carried by the beam, but also the amount of the power encircled in a given region of the transverse plane, or how much the beam profile is uniform. Yet, one could be interested in detecting the presence of vortices in the wavefront of a beam, or in evaluating the longitudinal distance along which the beam maintains some properties, i.e., for instance, its shape or some other features of its tranverse profile. As is obvious, the number of possible parameters farther grows if partially coherent, polarized and/or time varying light field are considered.

In the present Chapter we present some concepts, useful for characterizing light beams, which are of a very general nature, so that they can be applied to very wide classes of laser beams. In particular, the formalism of the beam moments will be shown, leading to the definition of a quality parameter that measures the propagation properties of a general light beam, as compared to those of a fundamental Gaussian beam, which is taken as the prototype of the "diffraction-limited" beam.

2.1 The width of a beam

One of the most widely used parameters for characterizing light beams is its *width*, or *diameter*. Nonetheless, a unique definition of the width for a general beam is still not accepted. In the case of Gaussian beams, the definition of spot-size stems from their well defined functional form so that they are said to have a finite width even though, from a mathematical point of view, their

profile fills the whole transverse plane. On the contrary, when the beam to be analyzed is not characterized by a precise functional form or when light beams of different types have to be compared, finding a unique definition of width seems not to be an easy task. In practice, several definition of width are used, each of them arising from a particular technique used to measure it [6, 7, 8, 9].

However, any quantity used as the measure of the beam width should satisfy some requirements. For example, it should be detectable by a reasonably simple experimental procedure. Furthermore, it should be minimum for only one value of the longitudinal coordinate and, possibly, its behavior on propagation should be regular enough.

A possible definition of width (Percent of Peak) is given by the radial coordinate in correspondence of which the intensity of the beam is reduced by a given factor, say η, typically $\eta = 1/e^2$ (see Fig. 1). In formulas, the width W is such that

$$I(r = W/2) = \eta I_{max} \, . \tag{21}$$

In the case of a Gaussian beam having spot size w, the width turns out to be $W = 2w$ (with $\eta = 1/e^2 = 13.53\%$).

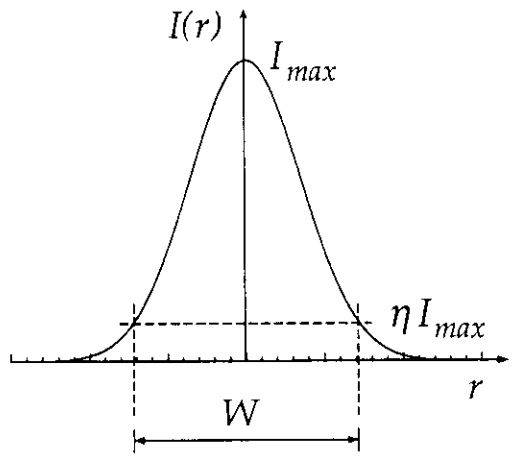

Figure 1: Definition of width in terms of Percent of Peak

Although such definition could be extended to asymmetric beams on in-

troducing two different widths along two orthogonal axes, it makes sense only if the beam intensity is symmetric enough and does not present significant angular oscillations.

A very used variant of the previous definition (Zero Width Slit) makes use of the value of the intensity integrated on thin stripes, instead of those of the intensity itself (Fig. 2).

$$\int_{-\infty}^{\infty} I(W/2, y)\ \mathrm{d}y = \eta \int_{-\infty}^{\infty} I(x_{\mathsf{peak}}, y)\ \mathrm{d}y\ . \tag{22}$$

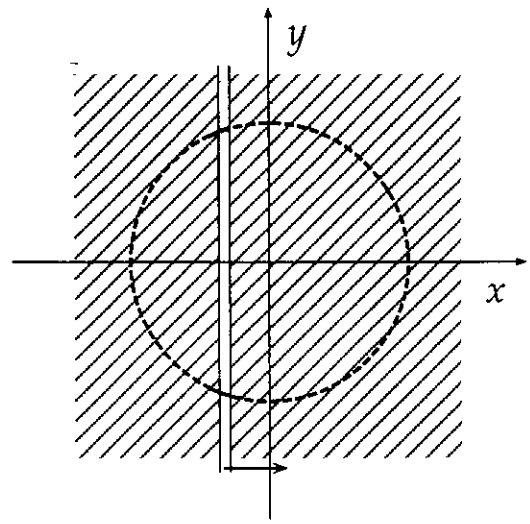

Figure 2: Zero Width Slit definition of width

In this way not only it is possible to define a width for any axis in the transverse plane, but the integration process also reduces the irregularities of the beam profile. Furthermore, the experimental determination of the width is simpler. On the contrary, some problems arise from the fact that a finite width of the stripe gives rise to a convolution of the actual intensity profile with a rect function.

A different definition (Variable Aperture Diameter) uses the values of the power transmitted by an aperture centered on the beam axis (see Fig. 3).

More precisely, the beam width is defined starting from the radius of the circular area in which a given fraction, say η, of the incident power falls. In formulas, we have

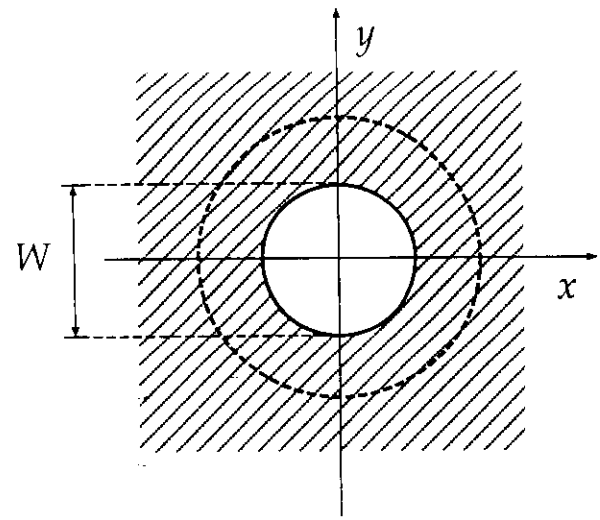

Figure 3: Variable Aperture Diameter definition of width

$$\int\limits_{r\leq W/2} I(\mathbf{r},z)\,\mathrm{d}^2r = \eta P_{\mathrm{tot}}\ , \tag{23}$$

where the integration domain is the circle of radius $W/2$, centered at the origin. When $\eta = 86.5\%$ and we consider the same Gaussian beam as above, this definition gives $W = 2w$ again. From an experimental point of view, some problems arise form the difficulties of a correct centering of the beam on the aperture. Furthermore, asymmetries of the profile are hardly detected.

The last definition we give in this Section is the one (Knife-Edge) based on the power that is transmitted when the beam impinges on an opaque half-plane, parallel to one of the axes, say y, of the transverse plane (Fig. 4). The half-plane is shifted along the x-axis and two positions are detected, for which the value of the transmitted power is equal to some given fractions η of the total power (typically 10% and 90%, respectively), i.e.,

$$\int_{-\infty}^{\infty}\mathrm{d}y\int_{x_0}^{\infty} I(x,y)\mathrm{d}x = \eta P_{\mathrm{tot}}\ . \tag{24}$$

The distance between these two positions furnishes a measure of the width of the beam along the x-axis. In order for the obtained value to be comparable to the ones given by the previous definitions. the distance between the two x-positions must be multiplied by a suitable factor, whose value depends

on the shape of the profile. For a nearly-Gaussian profile, for example, the moltiplication factor is 1.561.

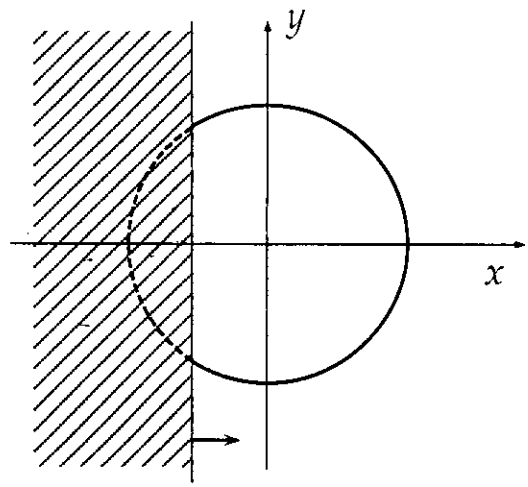

Figure 4: Knife-Edge definition of width

Modern beam-analysis systems often use solid-state image detectors. In such cases, intensity profiles are acquired, digitalized, and postprocessed, so that any of the above techniques can be emulated numerically. The main drawback is due to the possible presence of noise on the intensity data, but it can be reduced by suitable numerical a posteriori techniques.

In the following Section, we will give a further definition of width, which is particularly fit for characterizing light beams and is governed by very simple and general analytical expressions during propagation. Due to these reasons, despite some problems connected to its evaluation, it seems that it will become the standard definition of the width of a light beam.

2.2 Moments of a beam

A very efficient way for characterizing transverse profiles of a laser beam consists in using the *moments* of the intensity distribution , which are defined as for the case of probability distributions [10]. In fact, for any given transverse intensity profile $I(x, z)$, the following quantities can be defined:

$$\mu_n = \frac{1}{P_{tot}} \int x^n I(x,z)\mathrm{d}x \ . \tag{25}$$

For simplicity, here and in the following we shall limit ourselves to consider twodimensional beams, i.e., beams whose profile depends only on one of the transversal coordinates, say x. The extension of the obtained results to the case of threedimensional beams will be treated later.

Of course, assigning μ_n for any value of n is tantamount to specifying the intensity profile of a light beam in an unambiguous way. Nonetheless, as we shall see, lowest-order moments are often sufficient to characterize the main properties of a beam. The first-order moment, for instance, that is

$$\bar{x}(z) = \mu_1 = \frac{1}{P_{tot}} \int x I(x,z)\mathrm{d}x \ , \tag{26}$$

is the so called *centroid* and specifies the "center of mass" of the profile, while the second-order moment is related to the new definition of width we mentioned above. The width of a beam at the transverse plane z =const, in fact, is defined as proportional to the standard deviation of the intensity distribution $I(x,z)$, that is

$$\sigma(z) = \sqrt{\frac{1}{P_{tot}} \int [x - \bar{x}(z)]^2 \, I(x,z)\mathrm{d}x} \ . \tag{27}$$

In the following, for convenience, we shall refer to the standard deviation (27) as the width of the beam, neglecting the proportionality factor, which, to make the comparison possible with the previous definitions, is chosen as 4 (i.e., $W = 4\sigma$). We recall that the square modulus of the standard deviation is generally referred to as the variance of the distribution.

Of course, in order for Eq. (27) to be meaningful, it is not sufficient that the beam carries a finite energy, but it is required that the integral in the right-hand side of that equation is nondiverging. This is actually one of the most serious drawbacks of the definition of width based on intensity moments. In some significant cases, indeed, such as the far-field distribution produced by a slit or a circular hole, the integral in (27) cannot be evaluated. Actually, it diverges whenever the intensity profile is produced by diffraction of a field presenting discontinuities, in which cases the standard deviation of the profile cannot be defined.

Furthermore, even with well behaving intensity distributions some difficulties still remain, because the presence of the noise on the intensity data

can alter the value of the integral in a significant way. For this reason, several techniques have been proposed to suitably limit the integration domain an to reduce the effects of noise in width measuremets [6, 7, 8, 9].

For a fundamental Gaussian beam, the relationship between width and spot size can be easily deduced, and turns out to be

$$\sigma(z) = \frac{1}{2} w(z) \,. \tag{28}$$

Higher-order moments can be used to characterize the shape of an intensity profile. The best-known shape parameter is the so called *Kurtosis*, defined as [11]

$$K(z) = \frac{\frac{1}{P_{tot}} \int [x - \bar{x}(z)]^4 \, I(x,z) \mathrm{d}x}{\sigma^4(z)} \,, \tag{29}$$

which gives a quantitative measure of the flatness of a profile. It is 3 for "mesokurtic" beams (such as the fundamental Gaussian beam), it is less than 3 ("platykurtic") when the profile is flatter, and is greater than 3 ("leptokurtic") when the profile is sharper than a Gaussian one with the same variance. Three examples are shown in Fig. 5.

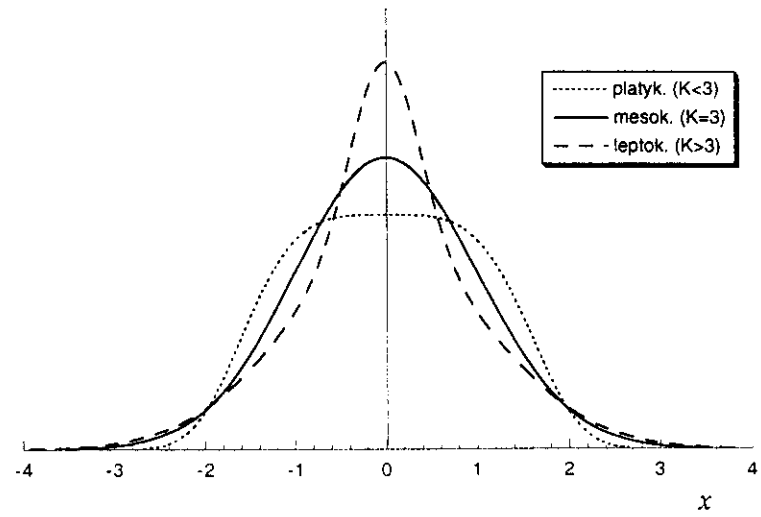

Figure 5: Three examples of intensity distribution having different kurtosis. Values of the total power and the variance are the same for the three cases.

2.3 Propagation of moments

Up to now, moments of the intensity profiles have been defined at a fixed transverse plane and, of course, they cannot give any information about the propagation features of the beam. A more complete characterization of the beam on propagation can be obtained by intruducing the moments of the intensity profile in the far field. By recalling that the far-field intensity is evaluated through the Fourier transform of the field at a plane z =const [2], we let

$$I_{\mathrm{ff}}(p) = \left| \int \psi(x,z) \exp(-i2\pi px) \mathrm{d}x \right|^2 , \tag{30}$$

where p is the variable conjugated to x and therefore is related to the angular variable individuating one direction across the plane (x,z). More precisely, $\vartheta_p = \lambda p$ is the angle between a typical direction and the z-axis. The same moments introduced above can now be defined for the far-field intensity. In particular, we have

$$\bar{p} = \frac{1}{P_{tot}} \int p I_{\mathrm{ff}}(p) \mathrm{d}p , \tag{31}$$

which gives the average propagation direction of the beam. The normalization factor is still P_{tot} because, from the Parseval theorem [12],

$$\int I_{\mathrm{ff}}(p) \mathrm{d}p = \int I(x,z) \mathrm{d}x , \tag{32}$$

as it should be evident from the energy conservation.

It can be easily shown, as a consequence of Eqs. (26) and (31), and from the Fresnel propagation formula, that the position of the centroid is a linear function of the longitudinal coordinate z:

$$\bar{x}(z) = \bar{x}(z_0) + \lambda \bar{p}(z - z_0) . \tag{33}$$

This means that the centroid of a light beam exactly follows the same propagation law which is valid for a ray in ray optics.

This fact allows us to choose a reference frame such that the propagation axis of the beam centroid coincides with the z−axis. In such a case, indeed, all first-order moments (both in the near and in the far field) vanish, i.e.,

$$\bar{x}(z) = \bar{p} = 0 \qquad \forall z , \tag{34}$$

and the evaluation of higher-order moments is simplified.

On exploiting condition (34), the variance of the far-field distribution turns out to be

$$\sigma_{\rm ff}^2 = \frac{1}{P_{tot}} \int p^2 I_{\rm ff}(p) {\rm d}p \ , \tag{35}$$

and is related to the average divergence angle of the beam $\vartheta = \lambda \sigma_{\rm ff}$. For the fundamental Gaussian beam having waist size $w(z_0)$, Eq. (35) gives

$$\sigma_{\rm ff} = \frac{1}{2\pi w(z_0)} \ . \tag{36}$$

As for the centroid, also the variance of the intensity profile takes a very simple form on paraxial propagation. In fact, it is not difficult to show that, for *any* paraxial beam, the following relation holds:

$$\sigma^2(z) = \sigma^2(z_0) + \lambda^2 \sigma_{\rm ff}^2 (z - z_0)^2 \ , \tag{37}$$

where $z = z_0$ is the plane where the width of the beam is minimum (waist plane). We will discuss this result in more detail in the following. Now, we only stress that Eq. (37) is formally identical to the law governing the variation of the spot size of a Gaussian beam [Eq. (11)].

The few results obtained in this Section may give an idea of how appealing could be the use of the moments formalism for the characterization of light beams.

2.4 The M^2 factor

In the previous Section we saw that the variance of a general light beam on paraxial propagation follows the same quadratic law valid for the spot size of a Gaussian beam. For convenience, we report here the law for the propagation of the width of a Gaussian beam [Eq. (11)], were the standard deviation σ is used instead of w:

$$\sigma^2(z) = \sigma^2(z_0) + \left[\frac{\lambda}{4\pi\sigma(z_0)} \right]^2 (z - z_0)^2 \ . \tag{38}$$

On comparing Eq. (38) to Eq. (37), we note that the only difference is that, in the latter, the coefficient of the quadratic term in z depends on the far-field width $\sigma_{\rm ff}$. This, in turn, not only depends on the width of the beam

at the waist plane, as in the case of a Gaussian beam, but it takes also into account the shape of the beam profile.

From the values of the widths of the beam at the waist and in the far field, the so called M^2 *factor* can be introduced, as the quantity [13, 14, 15]

$$M^2 = 4\pi\sigma(z_0)\sigma_{\rm ff} \ , \tag{39}$$

whence the propagation law (37) takes the form

$$\sigma^2(z) = \sigma^2(z_0) + \left[\frac{M^2\lambda}{4\pi\sigma(z_0)}\right]^2 (z - z_0)^2 \ . \tag{40}$$

The M^2 factor is 1 only for the fundamental Gaussian beam [see Eqs. (28) and (36)], while is greater than 1 for any other kind of beam. The average diffraction angle (ϑ) of the beam, shown in Fig. 6, turns out to be M^2 times greater than the equivalent angle for a fundamental Gaussian beam with the same waist width, i.e.,

$$\vartheta = M^2\vartheta_g \ . \tag{41}$$

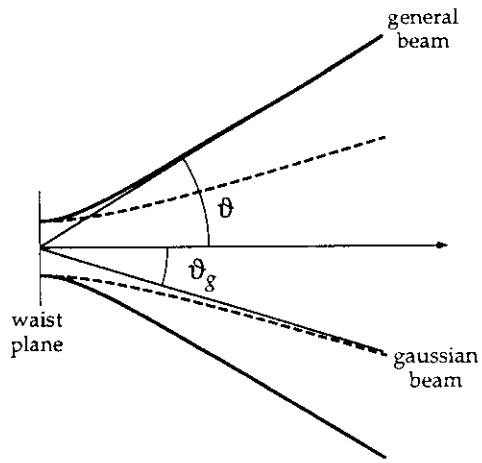

Figure 6: Sketch of the propagation of the width of a general light beam, compared to that pertinent to a fundamental Gaussian beam having the same variance at the waist.

The M^2 factor is generally used as a figure of the *quality* of a light beam, in that it measures the spreading attitude of a beam, once the waist width has been fixed. This is why it is often referred to as the "quality factor", or more properly, the "propagation factor" of a beam.

The fact that the M^2 factor cannot assume values less than 1 has a famous counterpart in Quantum Mechanics with the celebrated Heisenberg's uncertainty principle [16]. In fact, for any given wavefunction of a particle in the position representation, say $\psi_x(x)$, the variance of the probability distribution is evaluated as [16]

$$(\Delta x)^2 = \int |\psi_x(x)|^2 (x - \bar{x})^2 \, \mathrm{d}x \, . \tag{42}$$

Yet, the wavefunction in the momentum representation $\psi_p(P)$, can be used to evaluate the analogous variance of the probability distribution of the momentum P:

$$(\Delta P)^2 = \int |\psi_p(P)|^2 (P - \bar{P})^2 \, \mathrm{d}P \, . \tag{43}$$

The Heisemberg's uncertainty principle states that, for any quantum particle, the following disequality must hold:

$$\Delta x \, \Delta P \geq \frac{h}{4\pi} \, . \tag{44}$$

with h the Planck's constant, or, equivalently,

$$4\pi \Delta x \, \Delta \left(\frac{P}{h} \right) \geq 1 \, . \tag{45}$$

Actually, Eq. (44) is a consequence of the properties of the Fourier transform [12]. Indeed, the wavefunctions in the two representations are related to each other by the following relationship [16]:

$$\psi_p(P) = \frac{1}{\sqrt{h}} \mathcal{F} \{ \psi_x \} \left(\frac{P}{h} \right) \, , \tag{46}$$

and therefore a perfect analogy exists between the wavefunction of a quantum particle in the position representation and the function describing an optical field, as well as between the wavefunction in momentum representation and the far-field light field. Following this analogy, it is not difficult to recognize the M^2 factor in the left-hand side of Eq. (45).

Although the use of the M^2 factor as a figure of the quality of a light beam is more and more frequent and it can be often found on datasheets of laser sources, some researchers still look suspiciously at it. Main objections stem from the fact that it is defined in terms of second-order moments, whose measurement is often somewhat problematic. Moreover, as we saw above, the variance of a beam profile may diverge in rather frequent experimental conditions. For instance, when a beam suffers diffraction from an hard edge, the value of its M^2 diverges, while its "quality" may often be considered not so bad from a practical point of view.

The origin of this anomalous behavior is in the fact that the formalism if the M^2 factor is based on the formulas of paraxial propagation, while the presence of hard edges inavoidably introduces very high frequencies in the Fourier spectrum of the beam, which are responsible for the diverging behavior of σ_{ff}. Actually, any divergence is eliminated if the integrals in the Fourier domain are evaluated on a finite region [17, 18]. For instance, a truncation in correspondence of $|p| < 1/\lambda$, i.e., within the homogeneous region, is quite reasonable because evanescent components do not contribute to the far-field profile [19]. Nonetheless, the utility of the M^2 factor is still rather debated [20].

Before ending this Section, we quote a very important property of the M^2 factor: it is invariant after propagation through any paraxial optical system. So, we can say that it represents an intrinsic characteristic of a light beam, regardless the optical systems it passes through. Such a property is generally exploited in the experimental determination of M^2, where some values of the beam width are taken at different transverse planes and a fitting procedure is used to find the coefficients of their parabolic behavior. If the beam is well collimated, however, it must pass through an optical system (even a simple converging lens) to make the width variations more evident.

2.5 The embedded Gaussian beam

As we saw in the previous Sections, Eq. (40) is identical, except for the presence of M^2, to the expression governing the variance of a fundamental Gaussian beam. This fact suggests that one could associate, in some way, to any paraxial beam a fundamental gaussian beam, whose width is proportional to that of the beam under analysis at any transverse plane (see Fig. 7).

To this aim, it is sufficient to divide both sides of Eq. (40) by M^2 and set $\sigma_e(z) = \sigma(z)/\sqrt{M^2}$. We then obtain

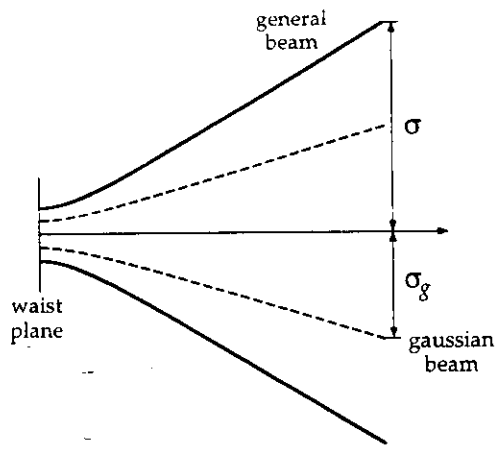

Figure 7: Sketch of the propagation of the width of a typical light beam (solid) together with the one pertinent to a fundamental Gaussian beam (dashed). The waist size of the latter is chosen in such a way to be proportional to that of the general beam at any tranverse plane.

$$\sigma_e^2(z) = \sigma_e^2(z_0) + \left[\frac{\lambda}{4\pi\sigma_e(z_0)}\right]^2 (z - z_0)^2 \,, \tag{47}$$

which is exactly the law valid for a fundamental Gaussian beam whose waist size is $\sigma_e(z_0)$. Following Eq. (28), the spot size of this Gaussian beam is

$$w_e(z_0) = 2\sigma_e(z_0) = \frac{2\sigma(z_0)}{\sqrt{M^2}} \,. \tag{48}$$

Such condition guarantees that the spot size of the Gaussian beam remains proportional to the width of the real beam at any transverse plane, the proportionality factor being $2/\sqrt{M^2}$. This Gaussian beam is referred to as the *embedded Gaussian beam* (EGB. for short) and represents a very useful tool for studying the propagation of light beams passing through paraxial optical systems [14, 21].

Before exposing the reasons of the importance of the EGB, we introduce a new quantity characterizing a beam profile: its *equivalent curvature radius.* As may be easily understood, the latter corresponds to the parabolic curvature radius fitting the real wavefront of the beam at its best. It can used, for

instance, to determine the focal length of the lens needed to collimate the beam. From an analytical point of view, it can be shown that the equivalent curvature radius is expressed, at any transverse plane, by the relation [22]

$$\frac{1}{R_e(z)} = 2\pi\lambda \frac{\int x \mathrm{Im}\left\{\psi^*(x,z)\partial_x\psi(x,z)\right\}\mathrm{d}x}{\int x^2 I(x,z)\mathrm{d}x} = \frac{2\pi\lambda}{P_{tot}\sigma^2(z)} \int x \mathrm{Im}\left\{\psi^*(x,z)\partial_x\psi(x,z)\right\}\mathrm{d}x \,. \tag{49}$$

A very remarkable property of the equivalent curvature radius is that on paraxial propagation it follows the same law as the curvature radius of a Gaussian beam, that is

$$R_e(z) = (z - z_0)\left\{1 + \left[\frac{4\pi\sigma^2(z_0)}{M^2\lambda\,(z - z_0)}\right]^2\right\} \,. \tag{50}$$

More precisely, how it is evident from Eqs.(50) and (48), it coincides with the curvature radius of the EGB.

This fact allows one to replace, to any real beam, its EGB to study its propagation through paraxial optical systems, if a description in terms of second-order moments is required. In these cases, indeed, it is sufficient to know position and width of the beam waist (or width and equivalent curvature radius at a general transverse plane) together with the M^2 factor, to recover the width after the passage through any paraxial optical system, as is sketched in Fig. 8. To this aim, the technique based on the complex curvature radius, recalled in Sect. 1.2, is particularly convenient. In passing, note that a general beam is completely specified (up to the second-order moments) by three parameters.

Before ending this Section, we report a useful formula relating the second-order moments of a beam at a general transverse plane:

$$\sigma^2(z) = (z - z_0)\,\lambda^2\sigma_{\mathrm{ff}}^2 R_e(z) \,. \tag{51}$$

2.6 Moments of the Wigner distribution function

A very compact and unifying approach to the parameters introduced in the previous Sections can be given in terms of the so-called *Wigner distribution*

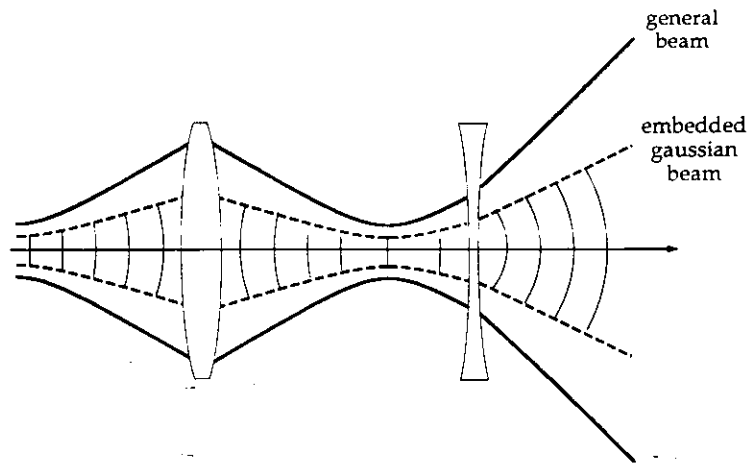

Figure 8: Example of beam propagation through a paraxial optical system. Solid curves refer to the behavior of the standard deviation of the tranverse profile of a typical light beam. Dashed curves shows the analogous quantity for the pertinent Embedded Gaussian Beam.

function (WDF) [23]. Limiting ourselves to the case of perfectly coherent twodimensional fields, the WDF of a light beam at the plane z =const is defined as [24]

$$W(x,p,z) = \int \psi(x+\xi/2,z)\psi^*(x-\xi/2,z)\exp(-i2\pi p\xi)\mathrm{d}\xi \ . \qquad (52)$$

It is a function of x and its conjugated variable p, simultaneously, so that it is said to give a representation of the beam in the space-frequency domain. The use of the WDF, borrowed from Quantum Mechanics [23], offers several advantages, mainly from a formal point of view, because if often leads to a very compact analytical description of phenomena related to paraxial propagation [6, 7, 8, 9]. Although we will not use the WDF formalism here, it is dutiful to mention it because it is the preferred tool of many researchers in this field.

All the quantities defined above can be introduced starting from the WDF. In particular, it can be easily seen that the integral of the WDF extended to the whole p-axis gives the optical intensity of the beam across the plane z =const, that is

$$\int W(x,p,z)\mathrm{d}p = I(x,z)\,, \tag{53}$$

while if the integral is summed on the x-axis, it gives the far-field intensity, i.e.,

$$\int W(x,p,z)\mathrm{d}x = I_{\mathrm{ff}}(p)\,. \tag{54}$$

Of course, the integral over the whole (x,p) plane is the total power carried by the beam, P_{tot}. It is also possible to define moments of any order as follows:

$$\mu_{nm} = \frac{1}{P_{tot}} \int x^n p^m W(x,p,z)\mathrm{d}x\mathrm{d}p\,. \tag{55}$$

First-order moments, μ_{10} and μ_{01}, represent the mean values of x and p, respectively.

The four second-order moments may be arranged in one 2×2 matrix:

$$\hat{V} = \frac{1}{P_{tot}} \int\int \begin{pmatrix} x^2 & xp \\ px & p^2 \end{pmatrix} W(x,p,z)\mathrm{d}x\mathrm{d}p\,, \tag{56}$$

which presents very interesting properties. When the reference frame is chosen in such a way that the first-order moments vanish, the elements V_{11} and V_{22} give the variances of the intensity at the plane z and in the far field, respectively. The diagonal term ($V_{12} = V_{21}$), after using some properties of the Fourier transform and of the Dirac delta function, can be written as

$$V_{12}(z) = \frac{2\pi}{P_{tot}} \int x\mathrm{Im}\left\{\psi^*(x,z)\partial_x\psi(x,z)\right\}\mathrm{d}x = \frac{\sigma^2(z)}{\lambda R_e(z)}\,, \tag{57}$$

where the definition of equivalent curvature radius (49) has been used.

Several useful relations can be derived from very general properties of the WDF [6, 7, 8, 9, 25]. For instance, it can be shown that the determinant of the matrix $\hat{V}$ is invariant under paraxial propagation and is related to the M^2 factor. Indeed, we have

$$\det\hat{V} = \sigma^2(z)\sigma_{\mathrm{ff}}^2 - \frac{\sigma^4(z)}{\lambda^2 R_e^2(z)} = \left(\frac{M^2}{4\pi}\right)^2\,, \tag{58}$$

where Eqs. (56), (57), (51), (37), and (39) have been used.

2.7 The three-dimensional case

The extension of the previously exposed ideas to the case of threedimensional beams does not present any further conceptual difficulties. However, the increase in the dimensionality leads to a much richer variety of beam types.

It is customary to divide light beams into three classes, depending on their symmetry properties [26, 9]. The simplest case is that of beams showing axial symmetry, both in amplitude and in phase. Such beams are referred to as *stigmatic* (ST) and, in particular, present the same values of the second-order moments along any direction across the transverse plane. It follows that, as for the twodimensional case, three parameters are sufficient for a complete, second-order characterization of the beam (for instance, position and width of the waist and M^2 factor).

A slightly more complicated type is that of *simple astigmatic* (SA) beams, for which it is possible to find a pair of orthogonal axes across the transverse plane, along which the beam behaves like a twodimensional beam. In particular, positions and widths of the two waists can be different from each other and, as a consequence, the curvature radius will be generally different along the two directions. The number of independent parameters needed to the second-order characterization of SA beams is 6, that is twice the parameters of a twodimensional beam.

The third class is that of *general astigmatic* (GA) beams, wich cannot be "decoupled" along two orthoigonal transverse axes. As an example, beams whose intensity profile rotates upon propagation without modifications of the transverse shape (the so-called "twisting beams" [27, 28, 29, 30]) belong to this class. Just to get an idea of a possible way to generate GA beams, we could think to a SA beam passing through a cylindrical lens, whose principal axes are rotated with respect to the axes of the incident beam by an angle different from 0 e da 90°, as it is shown in Fig. 9. It could be shown that the number of independent parameters of GA beams is 10 [9].

In the case of threedimensional beams it is still possible to define the second-order moments of the WDF, and arrange them in one matrix $\hat{V}$, with 4×4 elements:

$$\hat{V} = \frac{1}{P_{tot}} \int\int\int\int \begin{pmatrix} x^2 & xy & xp & xq \\ yx & y^2 & yp & yq \\ xp & yp & p^2 & pq \\ xq & yq & qp & q^2 \end{pmatrix} W(x,y,p,q,z)\mathrm{d}x\mathrm{d}y\mathrm{d}p\mathrm{d}q\,, \qquad (59)$$

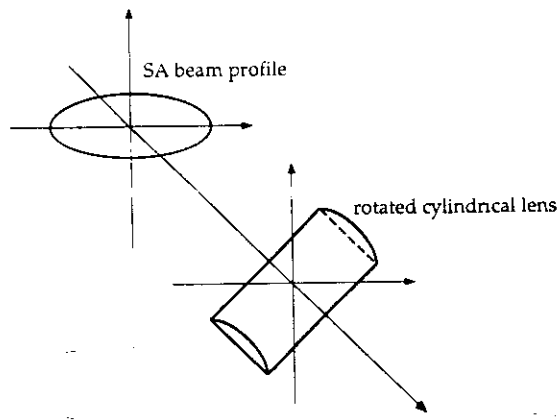

Figure 9: A possible scheme for generating GA beams, using a SA beam and a rotated cylindrical lens.

where q is the variable conjugated to y. Starting from the symmetry properties of $\hat{V}$, it can be shown that the number of independent parameters is 3, 6, and 10, for ST, SA, and GA beams, respectively [9].

In order to simplify the present exposition, in the following we shall limit ourselves to ST and SA beams. In these cases, the extension of the results given in the previous sections is quite trivial. For a ST beam, however, a different definition of M^2 is often used, which is based on the *radial* variance

$$\sigma_r^2(z) = \frac{\int_0^\infty I(r,z) r^3 \, \mathrm{d}r}{\int_0^\infty I(r,z) r \, \mathrm{d}r} \, . \tag{60}$$

Note that, since the profile is sopposed to be axially symmetric, it turns out that

$$\sigma_x^2(z) = \frac{\int\int I(x,y,z) x^2 \, \mathrm{d}x\mathrm{d}y}{\int\int I(x,y,z) \, \mathrm{d}x\mathrm{d}y} \, . = \frac{\int I(r,z) r^2 \, r\mathrm{d}r \int \cos^2\vartheta \, \mathrm{d}\vartheta}{2\pi \int I(r,z) \, r\mathrm{d}r} = \frac{1}{2}\sigma_r^2(z) \, . \tag{61}$$

Analogous symmetry properties must hold for the far-field pattern of a ST beam, so that the *radial* M^2 factor is defined as

$$M^2 = 2\pi\sigma_r(z_0)\sigma_{\mathrm{ff},r} \,. \tag{62}$$

where $\sigma_{\mathrm{ff},r}$ is the radial variance in the far field.

For the fundamental Gaussian beam having spot size $w(z)$, the definition of the radial variance leads to

$$\sigma_r(z) = \frac{w(z)}{\sqrt{2}} \,. \tag{63}$$

and to a value of the M^2 equal to 1 again.

2.8 Examples

Although the M^2 factor can be calculated for any paraxial beam, some cases exist for which it takes very simple analytical closed forms. Here, we see some examples.

Hermite–Gauss beams

Let us start from a twodimensional HG beam, whose expression is reported here for convenience:

$$\mathrm{HG_n}(x; v_0) = \left(\frac{2}{\pi v_0^2}\right)^{1/4} \frac{1}{\sqrt{2^n n!}} \exp\left[\frac{-x^2}{v_0^2}\right] H_n\left[\frac{x\sqrt{2}}{v_0}\right] \,. \tag{64}$$

The waist plane has been chosen as the plane $z = 0$ and we let $w(0) = v_0$. Normalization factors appearing in Eq. (64) have been introduced in order to obtain a unitary total power P_{tot}.

The variance of the beam profile at the waist is evaluated from Eqs. (27) and (64). After some calculations, we get

$$\sigma^2(0) = \frac{v_0^2}{2} \frac{\int x^2 H_n^2(x) \exp\left(-x^2\right) \mathrm{d}x}{\int H_n^2(x) \exp\left(-x^2\right) \mathrm{d}x} = \frac{v_0^2}{4}(2n+1) \,. \tag{65}$$

Intensity profiles of HG functions are shown in Fig. 10, together with the pertinent standard deviations.

The far-field variance has to be calculated starting from the squared modulus of the Fourier transform of the field (64). For a HG profile it can be

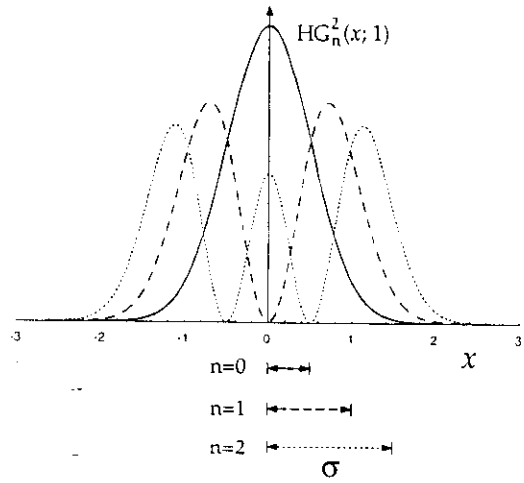

Figure 10: Transvere intensity profiles for some HG modes with $v_0 = 1$. Values of the pertinent standard deviation are also shown.

easily verified that, apart from a proportionality factor, its Fourier transform coincides with the profile itself, so that

$$\mathcal{F}\{\mathrm{HG}_n(x; v_0)\} = i^{-n}\mathrm{HG}_n(\sqrt{\pi}w_0 p) \,. \tag{66}$$

This fact is expressed by saying that HG functions belong to the class of the *self-Fourier* functions [31, 32]. As a consequence, the expression of σ_{ff}^2 is analogous to the one evaluated at the waist plane, and turns out to be

$$\sigma_{\mathrm{ff}}^2 = \frac{(2n+1)}{4\pi^2 v_0^2} \,, \tag{67}$$

whence the M^2 factor is

$$M^2 = (2n+1) \,. \tag{68}$$

It is 1 when $n = 0$ and increases with a linear law on increasing n. Furthermore, as was expected, the EGB of the $n-$th order HG beam is just the fundamental Gaussian beam having the same waist size v_0, as it is evident from Eqs. (68) and (48).

The present results are still valid for the $x-$ ($y-$)component of a three-dimensional HG beam.

Laguerre-Gauss beams

Since the profile is axially symmetric, we can evaluate the radial variances $\sigma_r^2(0)$ and $\sigma_{\mathrm{ff},r}^2$, and then the radial M^2 factor, too. Even in the case of LG beams, we can exploit the invariance of their profile under Fourier transformation (also LG function are self-Fourier functions), so that the evaluation of M^2 follows that of the previous example. In conclusion, we have, for a LG beams with indexes l and s,

$$M^2 = (2l + s + 1) \,, \tag{69}$$

and the quality of the beam get worse and worse on increasing the order of the beam.

Supergaussian beam

Another significant example is represented by beams having a flat-top profile at a given transverse plane. One of the (many) models used to describe such kind of beams is through the *supergaussian* function, defined as

$$\mathrm{SG}_\gamma(r; v_0) = \exp\left[-\left(\frac{r}{v_0}\right)^\gamma\right] \,, \tag{70}$$

which reduces to a Gaussian when $\gamma = 1$ and gives a profile more and more flattened on increasing γ (see Fig. 11).

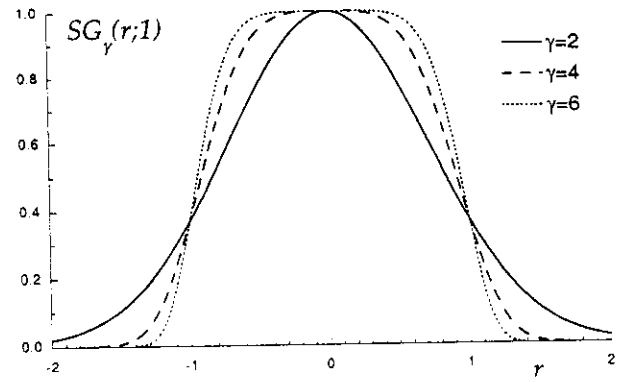

Figure 11: Supergaussian profiles with v_0=1. for different values of the parameter γ.

The M^2 factor of beams described by a field of the form (70) at the waist plane is [33]

$$M^2 = \frac{\gamma\sqrt{\Gamma(4/\gamma)}}{2\Gamma(2/\gamma)} , \tag{71}$$

with Γ the Gamma function [5], showing that the beam diffracts more and more on increasing the flatness of the profile. Plots of M^2 for different values of γ are reported in Fig. 12.

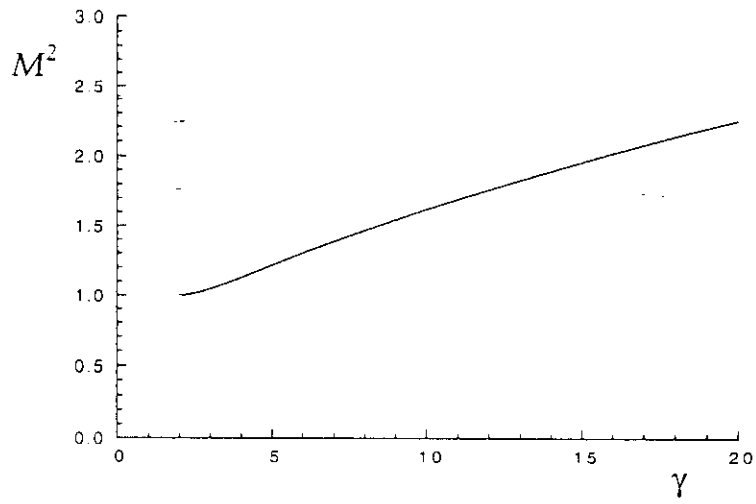

Figure 12: M^2 factor of supergaussian beams, as a function of the parameter γ.

Spherically aberrated Gaussian beam

It may be interesting to see how the M^2 factor gives account of aberration on the phase profile of a fundamental Gaussian beam. The case of spherical aberration leads to a particularly simple form of the M^2. In this case we can write the field emerging from an aberrated optical system as

$$U(r) = \exp\left(-\frac{r^2}{v_0^2} + i\frac{kr^2}{2R_0}\right)\exp\left(i\beta r^4\right) , \tag{72}$$

where β is related to the Seidel coefficient C_4 ($\beta = kC_4$), responsible for the spherical aberration [34].

Siegman showed [35] that for this kind of an aberrated beam, the M^2 factor takes the form

$$M^2 = \sqrt{1 + 2\beta^2 v_0^8}\,. \tag{73}$$

Plots of M^2 are reported in Fig. 13 as function of β, for different values of v_0.

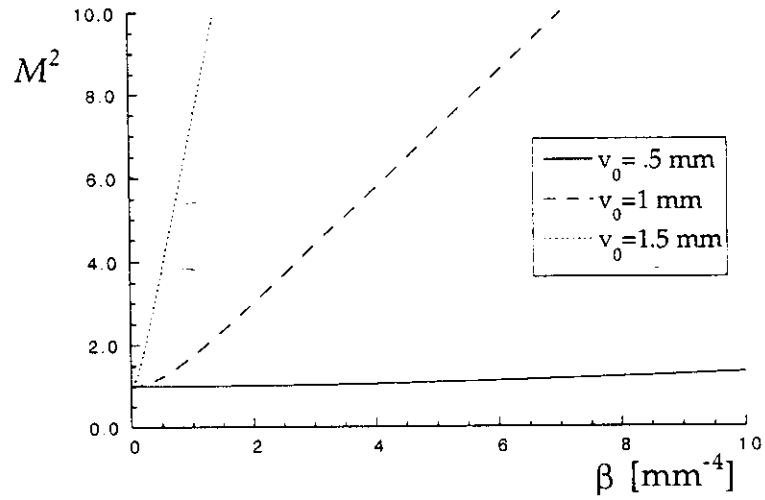

Figure 13: M^2 factor of a spherically aberrated fundamental Gaussian beam, as a function of the parameter β.

3 INCOHERENT MIXTURES OF GAUSSIAN MODES

In the previous Chapter, some aspects of the characterization of perfectly coherent light beams have been presented. What happens in practice, however, is that one has to deal with light beams that are only partially coherent, both from a spatial and from a temporal point of view. Due to these reasons, much research is currently carried to find out algorithms and experimental techniques devoted to a complete characterization of partially coherent beams.

One of the most significant results in this field is the extension of the concepts presented in the previous Chapter to the case of beams in any state of coherence. For these beams, in fact, it is still possible to define second-order moments, and then the M^2 factor, the embedded Gaussian beam, the equivalent curvature radius, and so on, following exactly the same procedures as for perfectly coherent light beams [6, 7, 8, 9, 36, 37]. Even in this case, the WDF, suitably defined starting from the cross-spectral density of the field, leads to the correct results in a very straightforward way [38].

In the present Chapter we dwell upon the study of a particular, but yet very important, class of partially coherent beams: the ones obtained as the output of a multimode laser cavity. More precisely, we will consider light beams obtained as the superposition of several transverse modes of a stable optical resonator with spherical mirrors. In such a case, if the mirrors are large enough and the elements present inside the cavity do not perturb significantly the resonator geometry, modes that can oscillate inside it are HG, or LG, modes [3]. So, in general, the beam emitted by a laser of this type can be modelled by a superpositionof higher-order Gaussian modes.

Under these hypotheses, it is quite reasonable to expect that the modes of the resonator have their waists at the same axial position, with the same spot-size, and propagate along the axis of the resonator. On the contrary, the power carried by each mode will strongly depends on the presence of obstacles inside the cavity and on the gain features of the active medium.

A more subtle question is whether the modes oscillate independently of one another, or they show mutual correlations. In principle, one cannot exclude that they could present some kind of correlation but, if they oscillate at different frequencies and measurements on the resulting beam are performed on time intervals longer that the beatment period, the modes can be considered, at least approximately, as completely uncorrelated. This is the

situation we will consider in the following.

It should be stressed, however, that sometimes a correlation among higher-order Gaussian modes must be taken into account. This is the case, for example, when one does not know the analytical form of the modes that really oscillate inside the cavity and uses a representation as the superposition of HG, or LG, functions with unknown coefficients. In this case, higher-order Gaussian modes represent only a mathematical basis to represent the actual modes and, of course, are supposed to be completely degenerate in frequency. Thus, even though the actual modes are uncorrelated from one another, this is not true for the Gaussian modes.

Given a multimode-laser beam, one of the problems one is often faced to is to determine the power content of each component mode. From this knowledge, indeed, it is possible to get all information not only about the propagation parameters of the beam (such as position and width of the waist, and M^2-factor), but also about its coherence properties [39, 40, 9]. In particular, it is possible to perfectly recover the mutual coherence function for any pairs of points in space. Furthermore, important information about the workimg conditions of the active medium can be gained [41].

In the Sections to follow, the problem will be based mathematically, and a procedure will be given for the determination of the modal weights starting from values of the beam intensity at a transverse plane [42, 43]. In doing so, we first limit ourselves to the twodimensional case, taking into account incoherent superpositions of modes of the HG_n type, whose waist is supposed to be known. Later, we will see that the extension to the threedimensionale case presents very serious problems. In this case, in fact, it becomes possible that different combinations of modal weights give rise to laser beams which are absolutely undistinguishable from an intensity basis, but yet present different physical properties, such as their coherence state.

3.1 Propagation parameters

Let us start from the expression of the disturbance of the nth HG mode at its waist [Eq. (64)]. The functions in Eq. (64) are normalized in the sense that

$$\int_{-\infty}^{+\infty} \mathrm{HG}_n^2(x; v_0)\mathrm{d}x = 1 \qquad \forall n \,. \tag{74}$$

Since the modes are supposed to oscillate indipendently from one another, they do not interfere in a stationary way. So, we can conclude that the

transverse intensity profile of the beam at the waist plane has the form

$$I(x) = \sum_{n=0}^{\infty} c_n \mathrm{HG}_n^2(x; v_0). \tag{75}$$

The c_n coefficients are positive coefficients and, thanks to Eq. (75), they can be thought of as the power content of each mode.

As a simple consequence of the knowledge of the modal weights c_n, we now evaluate the M^2 factor of a multimode laser beam [14]. To this aim, it is sufficient to calculate the variances of the beam profile at the waist plane and in the far field, by exploiting the fact that the modes are supposed to be mutually incorrelated.

Starting from the expression of the transverse intensity [Eq. (75)] and using the definition of variance [Eq. (27)], we get

$$\sigma^2(0) = \frac{w_0^2 \sum_n c_n(2n+1)}{4 \sum_n c_n}, \tag{76}$$

where the expression of the variance of each HG mode [Eq. (65)] has been taken into account.

In an analogous way, from Eq. (67) the far-field intensity variance turns out to be

$$\sigma_{\mathrm{ff}}^2 = \frac{\sum_n c_n(2n+1)}{4\pi^2 w_0^2 \sum_n c_n}, \tag{77}$$

so that the M^2 factor turns out to be

$$M^2 = \frac{\sum_n c_n(2n+1)}{\sum_n c_n}, \tag{78}$$

i.e., it is given by the average value of the M^2 factors of each HG modes, weighted by the c_n coefficients. Therefore it is evident that, as far as the diffraction properties of the beam are concerned, the beam quality decreases on increasing the power content of higher-order modes.

The evaluation of the M^2 factor can be performed in a more easy and direct way by resorting to the properties of the embedded Gaussian beam.

In fact, since the spot size of all the component Gaussian modes widens following the same law and the modes do not interfere with one another, the embedded Gaussian beam must coincide with the component mode of zero order. Therefore,

$$w_e(0) = v_0 \,, \tag{79}$$

and, recalling Eq. (48), we can write

$$M^2 = \frac{4\sigma^2(0)}{v_0^2} \,, \tag{80}$$

which leads to the evaluation of the M^2 factor directly from the knowledge of the waist size of the modes and the variance of the beam width. The importance of Eq. (80), however, is in the fact that the spot size of the component modes can be recovered from the knowledge of the beam quality factor and of the variance of the intensity profile at a transverse plane.

3.2 The inversion algorithm

What we are going to obtain is a general tool to evaluate the set of c_n, once the intensity profile is known. The difficulty stems from the fact that, while the HG_n's constitute an orthogonal set, their squares obviously do not. Consequently, the usual scalar product rule that we would adopt for evaluating the coefficients of a series expansion into orthogonal functions cannot be applied. We can even wonder whether a unique solution exists for the c_n's. Surprisingly enough, it happens that on passing to the Fourier transform domain the coefficients can be evaluated by the scalar product rule. This may sound contradictory because the scalar product is conserved under Fourier transformation. As a matter of fact, the property we are going to exploit is slightly subtler. Substantially, it turns out that the Fourier transforms of the HG_n^2's, while not orthogonal on the whole p-axis (p being a spatial frequency variable), are indeed orthogonal on the half-axis $p \geq 0$ with respect to the variable p^2.

Some comments have to be made about the intensity profiles at transverse planes other than the waist plane. HG modes have the property that their transverse shape does not change under paraxial approximation, apart from phase factors and a scaling of the transverse coordinate, deriving from the propagation law for the spot-size of Gaussian beams. This implies that beams

obtained as incoherent superpositions of HG modes are shape invariant, i.e., the expression of their intensity distribution remains of the form (75) at any transverse plane, provided that the quantity v_0 is replaced by the spot-size, say v_z, of the modes at that plane [44]. Thus, we shall refer to Eq. (75) as our starting point.

Coming back to our problem, we first note that the following notable relation holds:

$$\mathcal{F}\left\{\mathrm{HG}_n^2(x; v_0)\right\}(p) = \Psi_n(\pi^2 v_0^2 p^2)\,, \tag{81}$$

where the functions

$$\Psi_n(t) = L_n(t)\exp\left(-\frac{t}{2}\right) \tag{82}$$

have been introduced, L_n being the nth order Laguerre polynomial. A very useful property of the Ψ_n functions is that they are orthogonal on the half-axis $t \geq 0$, i.e.,

$$\int_0^\infty \Psi_n(t)\Psi_m(t)\mathrm{d}t = \delta_{n,m}, \tag{83}$$

$\delta_{n,m}$ being the Kronecker symbol. This fact leads to a very simple procedure for recovering the weights c_n starting from values of the intensity.

First, by Fourier transforming both sides of Eq. (75) and using Eq. (81), we obtain

$$\tilde{I}(p) = \sum_{n=0}^{\infty} c_n \Psi_n(\pi^2 v_0^2 p^2)\,. \tag{84}$$

Then, by exploiting the orthogonality of the Ψ_n functions [see Eq. (83)], the following expression for the expansion coefficient c_n is found:

$$c_n = 2\pi^2 v_0^2 \int_0^\infty \tilde{I}(p)\Psi_n(\pi^2 v_0^2 p^2)\, p\,\mathrm{d}p\,. \tag{85}$$

This equation allows us to evaluate the power content of each mode starting from the knowledge of the spot-size of the modes and the Fourier transform of the transverse intensity profile of the beam. $\tilde{I}(p)$ can be obtained by Fourier transforming the intensity profile of the beam at a transverse plane. It is interesting to note that values of $\tilde{I}(p)$ for $p < 0$ do not affect the integral in Eq. (85). This is not surprising, because $I(x)$ is real and the Fourier transform of a real function is Hermitian, namely, $\tilde{I}(-p) = \tilde{I}^*(p)$. Thus, negative frequencies actually do not carry any further information with respect to the positive ones.

In the Sections to follow we will see some examples of application of Eq. (85) to cases of common interest.

3.3 Two examples

In the present Section, Eq. (85) is applied to two classes of partially coherent beams obtained as the incoherent superposition of HG modes and for which the distribution of the c_n coefficients has already been investigated. The first of them is the class of the so-called Gaussian Schell-model beams [45]. They are characterized by a transverse intensity distribution and a degree of spatial coherence [46] that are both Gaussian and represent the most celebrated example of partially coherent beams, due to both their simple analytical representation and their ability to model real laser beams [47, 49, 51, 52].

The second class is that of beams showing a flat-topped transverse intensity profile. Beams of this kind are encountered, for instance, as the output of high-power multimode lasers and their flatness has been related to saturation effects of the gain medium [41]. The mode distribution inside such cavities was first studied through a least-square optimization procedure [41], and later by means of an analytical approach based on the so called flattened Gaussian (FG for short) beams [60, 43].

3.3.1 Gaussian intensity distribution

Let us consider the profile

$$I(x) = I_0 \exp\left(-\frac{x^2}{2\sigma_I^2}\right), \tag{86}$$

with I_0 and σ_I positive parameters (see Fig. 14).

The Fourier transform of $I(x)$ can be easily evaluated, yielding

$$\tilde{I}(p) = I_0\sqrt{2\pi}\,\sigma_I \exp\left(-2\pi^2\sigma_I^2 p^2\right). \tag{87}$$

On substituting from Eq. (87) into Eq. (85), we obtain

$$\begin{aligned} c_n &= I_0\sqrt{2\pi}\,\sigma_I \int_0^\infty L_n(t) \exp\left[-\frac{t}{2}\left(1+\frac{4\sigma_I^2}{v_0^2}\right)\right] \mathrm{d}t \\ &= I_0\sqrt{\frac{\pi}{2}}\,\frac{\frac{v_0^2}{\sigma_I}}{\left[1+\left(\frac{v_0}{2\sigma_I}\right)^2\right]}\left[\frac{1-\left(\frac{v_0}{2\sigma_I}\right)^2}{1+\left(\frac{v_0}{2\sigma_I}\right)^2}\right]^n, \end{aligned} \tag{88}$$

$(n = 0, 1, 2, \ldots)$.

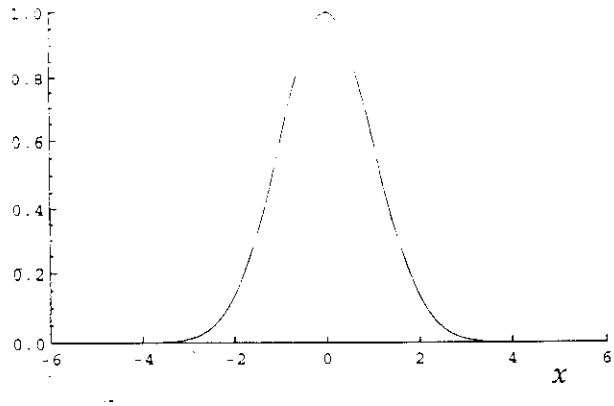

Figure 14: Intensity distribution $I(x)$ for a Gaussian Schell-model source with $I_0 = 1.$ and $\sigma_I = 1.$

where the variable $t = \pi^2 v_0^2 p^2$ has been introduced and use has been made of formula 7.414.6 of Ref. [48]. On defining the quantities

$$c_0 = I_0 \sqrt{\frac{\pi}{2}} \frac{\frac{v_0^2}{\sigma_I}}{\left[1 + \left(\frac{v_0}{2\sigma_I}\right)^2\right]}, \tag{89}$$

and

$$q = \frac{1 - \left(\frac{v_0}{2\sigma_I}\right)^2}{1 + \left(\frac{v_0}{2\sigma_I}\right)^2}, \tag{90}$$

the c_n coefficients can be written as

$$c_n = c_0 q^n, \qquad (n = 0, 1, 2, \ldots). \tag{91}$$

This is just the expression, derived by Gori [49] and Starikov and Wolf [50], for the expansion coefficients of a Gaussian Schell-model source (GSM), that is a source having degree of coherence given by

$$\mu(x_1, x_2) = \exp\left[-\frac{(x_1 - x_2)^2}{2\sigma_\mu^2}\right]. \tag{92}$$

where

$$\frac{1}{\sigma_\mu^2} = \frac{1}{4\sigma_I^2}\left[\left(\frac{2\sigma_I}{v_0}\right)^4 - 1\right]. \tag{93}$$

We note that the condition $\sigma_\mu^2 \geq 0$ implies that $v_0 \leq 2\sigma_I$ and, in turn, from Eqs. (90) and (91), that $c_n \geq 0$ for any n.

The behavior of the modal weights for several values of the parameter q are shown in Fig. 15, where the coefficients have been normalized according to the condition $\sum_n c_n = 1$.

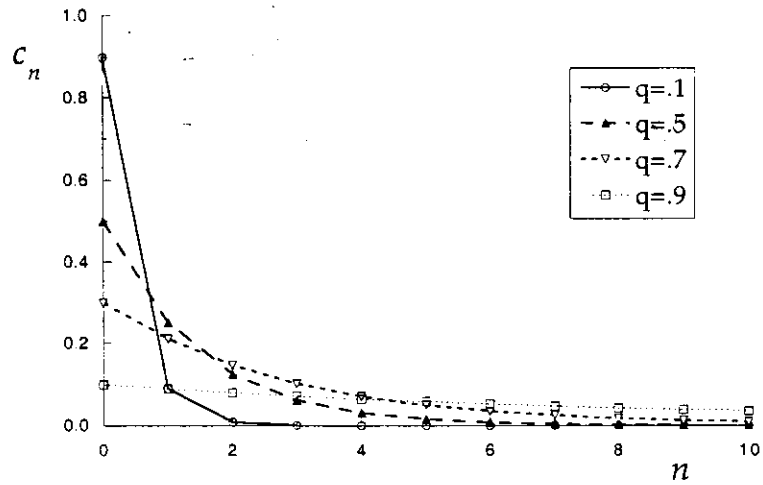

Figure 15: Normalized coefficients c_n for a Gaussian intensity profile for several values of the parameter q.

This example shows how, starting from the transverse intensity distribution of a beam, Eq. (85) leads to the complete characterization of the partially coherent beam.

Application of Eq. (80) to the present case gives at once

$$M^2 = \frac{4\sigma_I^2}{v_0^2}, \tag{94}$$

or, equivalently, on introducing the parameter σ_μ, which gives the width of the degree of coherence on the waist plane [see Eqs. (92) and (93)],

$$M^2 = \sqrt{1 + \frac{4\sigma_I^2}{\sigma_\mu^2}}. \tag{95}$$

This expression puts into evidence the contribution of the spatial-coherence properties of a beam to its propagation factor M^2.

3.3.2 Flat-topped intensity distribution

Among the various mathematical models used to describe flat-topped profiles [53, 54, 55], we choose the so-called flattened Gaussian (FG) model [54], which proved to be particularly fitted to study paraxial propagation of coherent flat-topped light beams [56, 57, 58, 59]. So, we start from an intensity profile of the form

$$I(x) = I_0 \exp\left[-\frac{(N+1)}{w_0^2}x^2\right] \sum_{n=0}^{N} \frac{1}{n!}\left[\frac{(N+1)}{w_0^2}x^2\right]^n . \tag{96}$$

Here N is a positive integer and w_0 is a real, positive parameter. w_0 and N are related to the width of the transverse region on which I is appreciably different from zero and to the rapidity of the transition from the maximum value to zero, respectively.

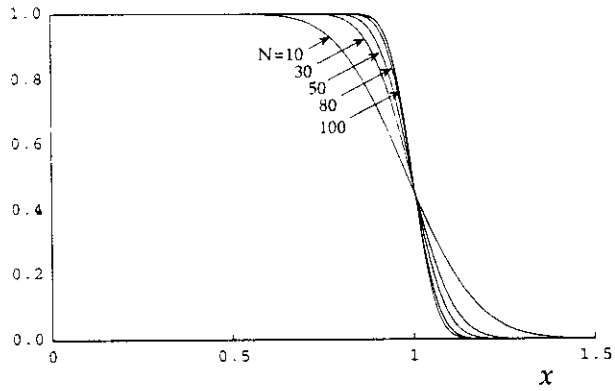

Figure 16: Flattened Gaussian intensity profiles for $w_0 = 1$, $I_0 = 1$, and several values of N

The intensity behavior, as a function of x, is shown in Fig. 16 for $w_0 = 1$, $I_0 = 1$, and several values of the parameter N.

It was shown in Ref. [60] that a precise relationship between w_0, N, and the spot-size of the underlying HG modes exists, that is

$$v_0 = w_0 \left(\frac{2}{N+1}\right)^{1/2} . \tag{97}$$

The Fourier transform of I can be evaluated analytically [43] and takes the simple form

$$\begin{aligned} \tilde{I}(p) &= I_0 \frac{(-1)^N}{\sqrt{\pi} 2^{2N+1} N! p} \\ &\times H_{2N+1}\left(\frac{\pi w_0 p}{\sqrt{N+1}}\right) \exp\left(-\frac{\pi^2 w_0^2 p^2}{N+1}\right). \end{aligned} \tag{98}$$

On inserting from Eq. (98) into Eq. (85) and taking Eq. (97) into account, after some manipulations we obtain

$$\begin{aligned} c_n &= I_0 w_0 \frac{(-1)^N}{2^{2N-1} N!} \left(\frac{2\pi}{N+1}\right)^{1/2} \\ &\times \int_0^\infty H_{2N+1}(\xi) L_n(2\xi^2) \exp(-2\xi^2) \mathrm{d}\xi. \end{aligned} \tag{99}$$

It can be easily shown that, due to the properties of Laguerre and Hermite polynomials [5], all c_n vanish if $n > N$.

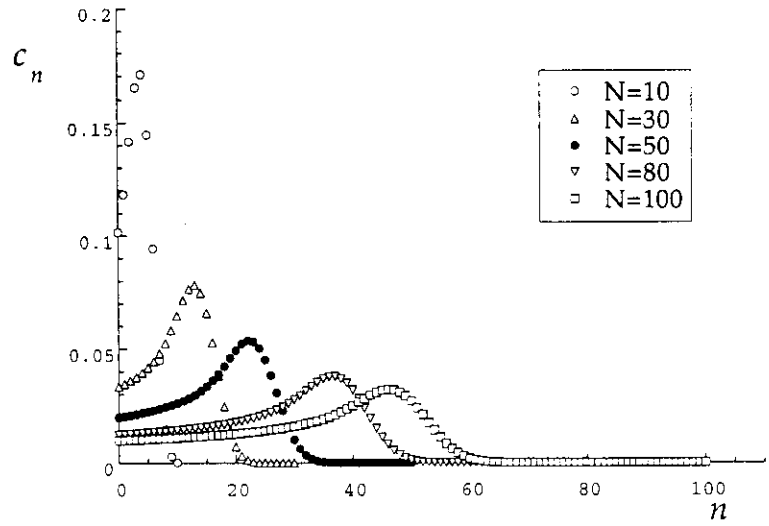

Figure 17: Normalized coefficients c_n for FG intensity profiles with several values of the order N.

Values of c_n, normalized according to the condition $\sum_n c_n = 1$, are shown in Fig. 17 for some values of the order N. They can be compared with

those derived in Ref. [60] using a different approach. Curves of the degree of spatial coherence are shown in Fig. 18 as a function of x_2, for different values of x_1 and N.

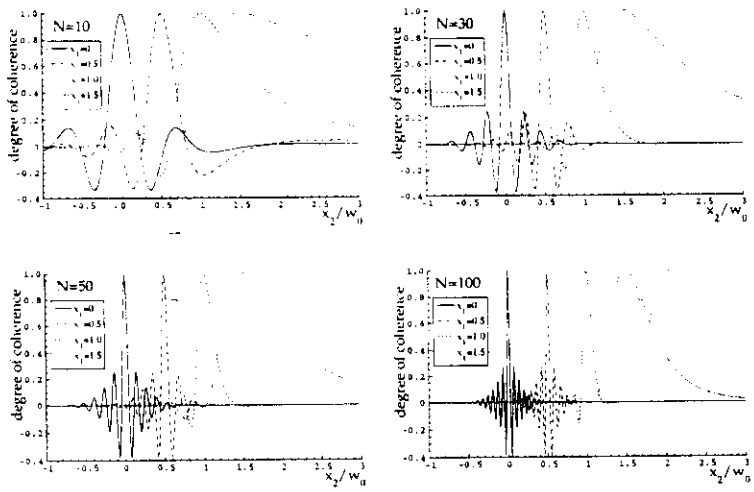

Figure 18: Curves of the degree of spatial coherence aa function of x_2, for different values of x_1 and N

In this case the evaluation of the M^2 factor yelds

$$M^2 = 1 + \frac{2}{3}N \,. \tag{100}$$

3.4 The three-dimensional case

Up to know, we considered incoherent superpositions of twodimensional higher-order Gaussian beams. We saw that, in such a case, for any given intensity profile of the resulting beam the set of the modal weights c_n is determined without any ambiguity, and a precise mathematical procedure exists to recover it. In the present Section. we give an example of a threedimensional case and we show that different combinations of c_n can give rise to identical intensity distributions. This means that it is no more possible, in general, to recover the power content of the modes starting from the sole values of the intensity of the resulting beam. This agrees with general results obtained from the properties of the cross-spectral density on paraxial propagation [61, 62]

As an example, we consider the superposition of two modes of the tytpe

$$V^{\pm}(r,\vartheta) = r\exp\left(-\frac{r^2}{v_0^2}\right)\exp\left(\pm i\vartheta\right) , \tag{101}$$

which coincides, apart from proportionality factors, to LG modes having indexes $l = 0$ e $s = \pm 1$ [see Eq. (20)].

The argument of the last exponential in Eq. (101) gives account of the helicoidal structure of the phase front of the modes. The only difference between the two modes is the sign of the argument, which implies that one of them skrews clockwise, while the other one in the opposite sense. Similar phase structures are known as *optical vortices* and the integer factor multiplying the variable ϑ (in these cases $+1$ and -1, respectively) is referred to as the *charge* of the vortex [63].

Although the two modes are physically different from each other, they give rise exactly to the same intensity profile, that is

$$I^{\pm}(r,\vartheta) = r^2\exp\left(-\frac{2r^2}{v_0^2}\right) . \tag{102}$$

The transverse pattern, shown in Fig. 19. justifies the name, *donut modes*, given to modes of the form (101).

When an incoherent superposition of such modes is considered, with weights c_+ and c_-, respectively, the intensity of the resulting beam is given by

$$I(r,\vartheta) = (c_+ + c_-)\, r^2\exp\left(-\frac{2r^2}{v_0^2}\right) , \tag{103}$$

and it is the same for all those cases for which the condition

$$c_+ + c_- = \text{const} \tag{104}$$

is met. Furthermore, since LG modes are shape-invariant on paraxial propagation, any incoherent superposition of LG modes will be shape-invariant as well, so that all beams obtained within condition (104) will present exactly the same intensity profile at any transverse plane. Therefore, they cannot be distinguished from one another on an intensity basis. Finally, it should be noted that profiles of the form shown in Fig. 19 can be also obtined by incoherently superimposing threedimensional HG modes (01 and 10 with the same power).

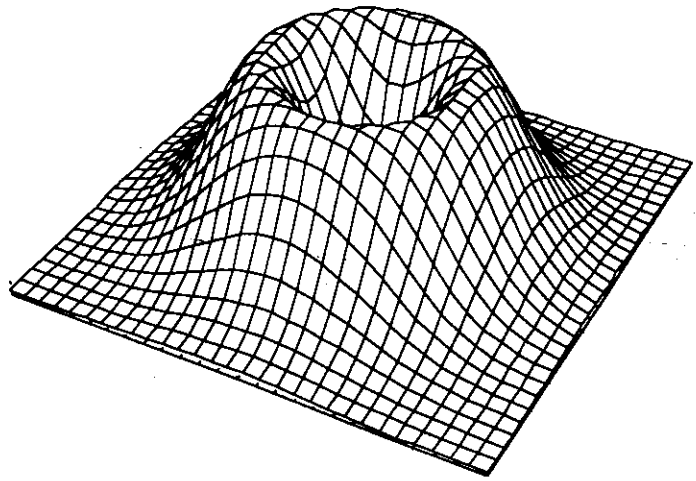

Figure 19: Intensity profile of a donut mode

It must be stressed that the difference among these beams is far from being only formal, and it has important consequences from the physical point of view. Actually, they differ in their coherence properties: It is sufficient to note, in fact, that the resulting beam is perfectly coherent when one of the modal weights vanishes but is only partially coherent in the other cases, as could be shown by explicitily evaluating its degree of coherence [62]. So, the only way to determine the modal weights is to perform coherence measurements on the beam [64, 39].

An example of this behavior is given in Refs. [66] and [65], where three-dimensional flat-topped beams with the same intensity distribution are obtained superimposing uncorrelated HG modes and LG modes, respectively.

Actually, such a situation is not limited to the case of superposition of LG

modes. but is encountered whenever the component modes present vortices in their phase profile. In such cases. the shape-invariance of the beam is generally lost. but the intensity profiles obtained within condition (104) are always undistinguishable from one another at any transverse plane [61, 67].

References

[1] M. Born and E. Wolf, *Principle of Optics*, (Pergamon, Oxford, 1993).

[2] JJ. W. Goodman *Introduction to Fourier Optics*, (McGraw Hill, New York, 1996).

[3] A. E. Siegman, *Lasers*, (University Science Books, Mill Valley, California, 1986).

[4] W. Brouwer, *Matrix Methods in Optical Instrument Design*, (Benjamin, New York, 1964).

[5] M. Abramowitz and I. Stegun, *Handbook of mathematical functions*, (Dover, New York, 1972).

[6] P. M. Mejías, H. Weber, R. Martínez-Herrero, and A. González-Ureña, Eds., Proc. Workshop on Laser Beam Characterization (SEDO, Madrid, 1993).

[7] H. Weber, N. Reng, J. Lüdtke, and P. M. Mejías, Eds., Laser Beam Characterization, (Festkörper-Laser-Institute GmbH, Berlin, 1994).

[8] M. Morin and A. Giesen, Eds., Third Internation Workshop on Laser Beam and Optics Characterization, Proc. SPIE **2870** (1996).

[9] A. Giesen and M. Morin, Eds., Proc. Fourth Internation Workshop on Laser Beam and Optics Characterization, (Institut für Strahlwerkzeuge, Munich, 1997).

[10] A. Papoulis, *Probability, Random Variables, and Stochastic Processes*, (McGraw Hill, New York, 1986)

[11] R. Martínez-Herrero, P. M. Mejías, ans G. Piquero, "Third- and fourth-order parametric characterization of partially coherent beams propagating through ABCD optical systems," Opt. and Quantum Electr. **24**, 1021 (1992)

[12] R. B. Bracewell, *The Fourier Transform and its Applications*, (McGraw Hill, New York, 1986)

[13] M. W. Sasnett, "Propagation of multimode laser beams," in *The Physics and Technology of Laser Resonators*, (Adam Hilger, New York, 1989)

[14] A. Siegman, "New developments in laser resonators," Proc. SPIE **1224**, 2 (1990).

[15] T. F. Johnston Jr., "M^2 concept Characterizes Beam Quality," Laser Focus World **173**, (1990).

[16] J. J. Sakurai, *Modern Quantum Mechanics*, (Addison Wesley, Reading, MA, 1985)

[17] M. A. Porras "Experimental investigation on aperture-diffracted laser beam characterization," Optics Commun. **109**, 5 (1993)

[18] C. Paré and P.-A. Bélanger, "Propagation law and quasi-invariance properties of the truncated second-order moment of a diffracted laser beam," Optics Commun. **123**, 679 (1996)

[19] P.-A. Bélanger, Y. Champagne, and C. Paré, "Beam propagation factor of diffracted laser beam," Optics Commun. **105**, 233 (1994)

[20] Y. A. Anan'ev, "Once again on the laser beam quality criteria," Optics and Spectroscopy **86**, 439 (1999)

[21] P.-A. Bélanger, "Beam propagation and the ABCD matrix," Optics Lett. **16**, 196 (1991)

[22] A. E. Siegman, "Defining the effective radius of curvature for nonideal optical beams," IEEE J. Quantum Electr. **27**, 1146 (1991)

[23] E. Wigner, "On the quantum correction for thermodynamic equilibrium," Phys. Rev. A **40**, 749 (1932)

[24] M. J. Bastiaans, "The Wigner distribution function applied to optical signals and systems," Optics Commun. **25**, 26 (1978)

[25] M. J. Bastiaans, "Second-order moments of the Wigner distribution function in first-order optical systems," Optik **88**, 163 (1991)

[26] J. A. Arnaud and H. Kogelnik, "Gaussian light beams with general astigmatism," Appl. Opt. **8**, 1687 (1969)

[27] J.Serna, P.M.Mejas and R.Martinez-Herrero, "Rotation of partially coherent beams propagating through free space," Opt. Quantum Electron. **24**, s873 (1992)

[28] R. Simon and N.Mukunda, "Twisted Gaussian Schell-model beams," J. Opt. Soc. Am. **10**, 95 (1993)

[29] A.T. Friberg, E. Tervonen and J. Turunen, "Interpretation and experimental demonstration of twisted Gaussian Schell-model beams," J. Opt. Soc. Am. **11**, 1818 (1993)

[30] S. Chávez-Cherda, G. S. McDonald, and G. H. C. New, "Nondiffracting beams: travelling, standing, rotating and spiral waves," Opt. Commun. **123**, 225 (1988)

[31] M.J. Caola, "Self-Fourier functions," J. Phys. A: Math. Gen. **24**, L1143 (1991)

[32] G. Cincotti, F. Gori, and M. Santarsiero, "Generalized self-Fourier functions," J. Phys. A: Math. Gen. **25**, L1191 (1991)

[33] A. Parent, M. Morin, and P. Lavigne "Propagation of super-Gaussian field distributions," Opt. Quantum Electron. **24**, 1071 (1992)

[34] W. T. Welford, *Aberration of Symmetric Optical Systems*, (Academic, New York, 1974)

[35] A. E. Siegman, "Analysis of laser beam quality degradation caused by quartic phase aberrations," Appl. Optics **32**, 5893 (1993)

[36] R. Simon, M. Mukunda, and E. C. G. Sudarshan, "Partially coherent beams and a generalized ABCD law," Opt. Commun. **65**, 322 (1988)

[37] F. Gori, M. Santarsiero, and A. Sona, "The change of width for a partially coherent beam on paraxial propagation," Opt. Commun. **82**, 197 (1991)

[38] M. J. Bastiaans, "Application of the Wigner distribution function to partially coherent light," J. Opt. Soc. Am. **3**, 1227 (1986)

[39] J. Turunen, E. Tervonen, and A. T. Friberg, "Coherence theoretic algorithm to determine the transverse-mode structure of lasers," Opt. Lett. **14,** 627-629 (1989).

[40] E. Tervonen, J. Turunen, and A. T. Friberg, "Transverse laser-mode structure determination from spatial coherence measurements: experimental results," Appl. Phys. **B49,** 409-414 (1989).

[41] A. E. Siegman and S. W. Townsend. "Output beam propagation and beam quality from a multimode stable-cavity laser," IEEE J. Quantum Electron., **29,** 1212-1217 (1993).

[42] F. Gori, M. Santarsiero, R. Borghi, and G. Guattari, "Intensity-based modal analysis for partially coherent beams with Hermite–Gaussian modes," Opt. Lett. **23,** 989-991 (1998).

[43] M. Santarsiero, F. Gori, R. Borghi, and G. Guattari, "Evaluation of the modal structure of light beams composed of incoherent mixtures of Hermite–Gaussian modes," Appl. Optics **38,** 5272 (1999)

[44] F. Gori, in *Coherence and Quantum Optics*, L. Mandel and E. Wolf eds.. (Plenum Press, New York). 363 (1984).

[45] E. Collett and E. Wolf, "Is complete coherence necessary for the generation of highly directional light beams?," Opt. Lett. **2,** 27 (1978).

[46] L. Mandel and E. Wolf, *Optical Coherence and Quantum Optics*, (Cambridge University Press, Cambridge, Massachusetts, 1995).

[47] P. Spano, "Connection between spatial coherence and modal structure in optical fibers and semiconductors lasers," Opt. Commun. **33,** 265(1980).

[48] I. S. Gradshtein and I. M. Ryzhik, *Table of Integrals, Series, and Products*, (Academic Press, New York, 1980).

[49] F. Gori, "Collett-Wolf sources and multimode lasers," Opt. Commun. **34,** 301 (1980).

[50] A. Starikov and E. Wolf. "Coherent-mode representation of Gaussian Schell-model sources and of their radiation fields," J. Opt. Soc. Am. **72,** 923 (1982).

[51] E. G. Johnson, Jr., "Direct measurements of the spatial mode of a laser pulse: theory." Appl. Opt. **25,** 2967 (1986).

[52] A. T. Friberg, E. Tervonen, and J. Turunen, "Interpretation and experimental demonstration of twisted Gaussian Schell-model beams," J. Opt. Soc. Am. A **11,** 1818 (1994).

[53] S. De Silvestri, P. Laporta, V. Magni, and O. Svelto, "Solid-state laser unstable resonators with tapered reflectivity mirrors: the super-Gaussian approach," IEEE J. Quantum Electron. **24**, 1172 (1988).

[54] F. Gori, "Flattened Gaussian beams." Opt. Commun. **107**, 335 (1994).

[55] C. J. R. Sheppard and S. Saghafi, "Flattened light beams," Opt. Commun. **132**, 144 (1996).

[56] V. Bagini, R. Borghi, F. Gori, A. M. Pacileo, M. Santarsiero, D. Ambrosini, and G. Schirripa Spagnolo,"Propagation of axially symmetric flattened Gaussian beams," J. Opt. Soc. Am. A **13**, 1385 (1996).

[57] M. Santarsiero, D. Aiello, R. Borghi, and S. Vicalvi, "Focusing of axially symmetric flattened Gaussian beams," J. Mod. Opt. **44**,633 (1997).

[58] R. Borghi, M. Santarsiero, and S. Vicalvi, "Focal shift of focused flat-topped beams," Opt. Commun. **154**, 243 (1998).

[59] D. Aiello, R. Borghi, M. Santarsiero, and S. Vicalvi, "The integrated intensity of focused flattened Gaussian beams," Optik **109**, 97 (1998).

[60] R. Borghi and M. Santarsiero, "Modal decomposition of partially coherent flat-topped beams produced by multimode lasers," Opt. Lett. **23,** 313 (1998).

[61] F. Gori, M. Santarsiero, and G. Guattari, "Coherence and space distribution of intensity," J. Opt. Soc. Am. A **10,** 673 (1993).

[62] V. Bagini, F. Gori, M. Santarsiero, G. Guattari, and G. Schirripa Spagnolo, "Space intensity distribution and projections of the cross-spectral density," Opt. Commun. **102,** 495 (1993).

[63] G. Indebetouw, "Optical vortices and their propagation," J. Mod. Opt. **40**, 73 (1993)

[64] G. Iaconis and I. A. Walmsley, "Direct measurement of the two-point field correlation function," Opt. Lett. **21**, 1783-1785 (1996).

[65] R. Borghi and M. Santarsiero, "Modal structure analysis for a class of axially symmetric flat-topped laser beams," IEEE J. Quantum Electr. **35**, 745-750 (1999).

[66] F. Gori, M. Santarsiero, R. Borghi, and S. Vicalvi, "Partially coherent sources with helicodal modes," J. Mod. Opt. **45**, 539 (1998)

[67] T. E. Gureyev, A. Roberts, and K. A. Nugent, "Partially coherent fields, the transport-of-intensity equation, and phase uniqueness," J. Opt. Soc. Am. A **12**, 1942-1946 (1995).

NON-DIFFRACTING LIGHT BEAMS

There are beams whose profile does not change during propagation (both in shape and in size):

$\rightarrow$ *non-diffracting* or *diffraction-free* beams.

- Is their behavior consistent with the laws of propagation?
- What about their second-order moments?
- Why do they seem to spread less than a fundamental Gaussian beam?

A two-dimensional example

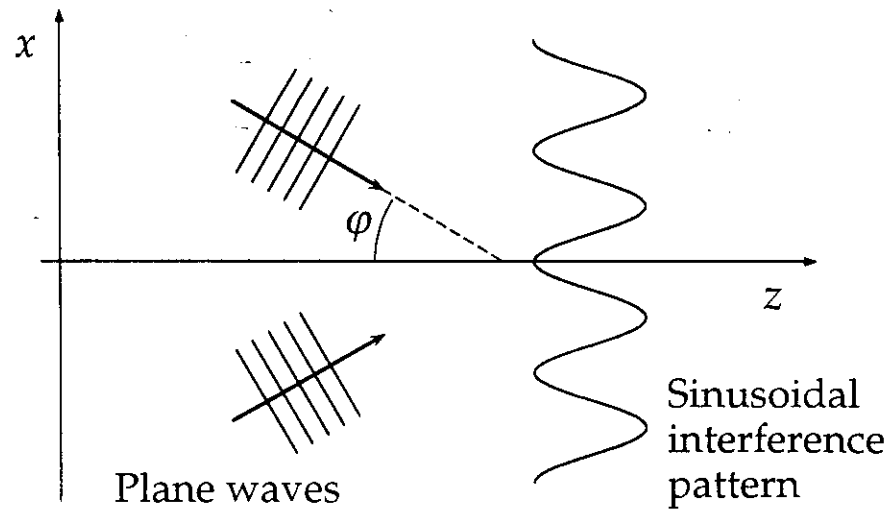

$$
\begin{aligned}
U(x,z) &= A\, e^{ik \sin\varphi\, x}\, e^{ik \cos\varphi\, z} \\
&\quad + A\, e^{-ik \sin\varphi\, x}\, e^{ik \cos\varphi\, z} \\
&= 2Ae^{ik \cos\varphi\, z} \cos(k \sin\varphi\, x)
\end{aligned}
$$

$$\Rightarrow I(x,z) = 4A^2 \cos^2(k \sin \varphi x)$$

The transverse intensity pattern does not depend on z

The two component plane waves suffer exactly the same dephasing along the z-axis:

$$e^{ik \cos \varphi z}$$

so that the interference pattern is the same, for any value of z (regardless of the values of the two amplitudes)

The three-dimensional case

We consider a superposition of plane waves. The only condition is that all of them have the same component k_z of the wavevector.

$\Rightarrow$ All wavevectors lie on a cone.

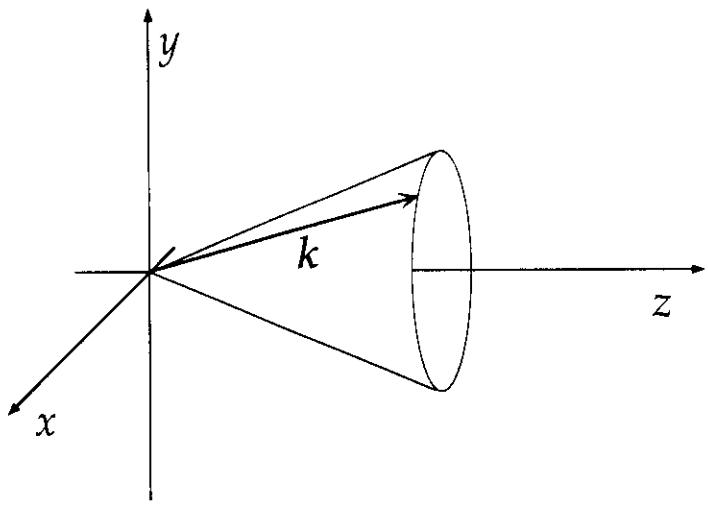

On the basis of what we saw in the two-dimensional case, we expect that the interference pattern will not change during propagation.

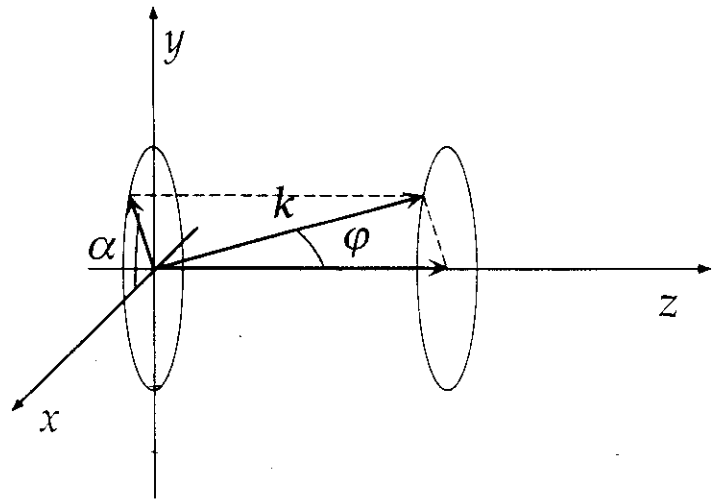

$$\mathbf{k} = k\ (\cos\varphi\,\hat{z} + \sin\varphi\cos\alpha\,\hat{x} + \sin\varphi\sin\alpha\,\hat{y})$$

so that a typical plane wave is written as

$$A(\alpha)e^{i\mathbf{k}\cdot\mathbf{r}} = A(\alpha)e^{ik\cos\varphi\, z}\ e^{ik\sin\varphi\ \cos\alpha\, x}\ e^{ik\sin\varphi\ \sin\alpha\, y}$$

or, in a cylindrical reference frame (r, ϑ, z),

$$A(\alpha)e^{i\mathbf{k}\cdot\mathbf{r}} = A(\alpha)e^{ik\cos\varphi\, z}\ e^{ikr\ \sin\varphi\ \cos(\vartheta-\alpha)}$$

Any (possibly continuous) superposition of such plane waves,

$$U(r, \vartheta, z) = e^{ik \cos\varphi\, z} \int A(\alpha)\, e^{ikr \sin\varphi \cos(\vartheta - \alpha)}\, \mathrm{d}\alpha$$

gives rise to a transverse intensity profile independent of z:

$$\Rightarrow I(r, \vartheta, z) = \left| \int A(\alpha)\, e^{ikr \sin\varphi \cos(\vartheta - \alpha)}\, \mathrm{d}\alpha \right|^2$$

for any choice of the weighting function $A(\alpha)$.

- Necessary and sufficient condition for a beam to be diffraction-free is that it can be expressed as a superposition of plane waves whose wavevectors lie on the surface of a cone.

The simplest case

If $A(\alpha) = A = \text{const}$:

$$U(r, \vartheta, z) = A\, J_0(\beta r)\, e^{ik \cos\varphi\, z} \qquad (\beta = k \sin\varphi)$$

$$= \underline{\text{Bessel beam}} \text{ of zero order}$$

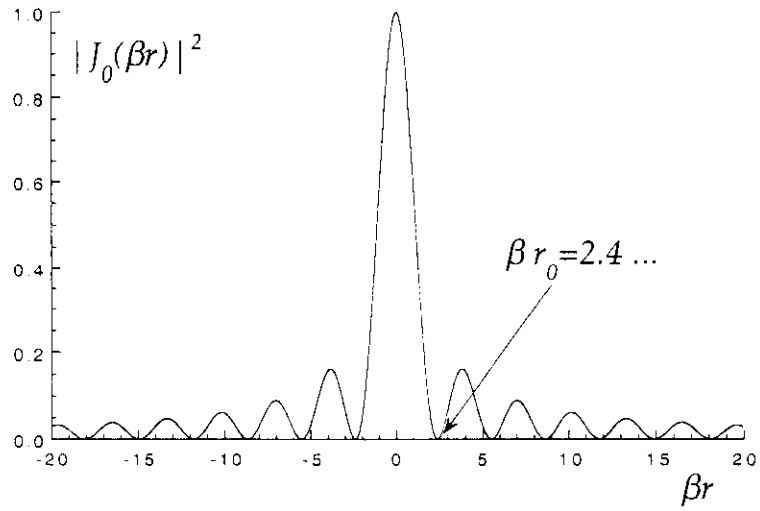

The size of the central lobe of the beam depends on λ and can assume values of the order of λ

(central-lobe diameter $\approx \lambda / \sin\varphi$)

Higher-order members

If we take $A(\alpha) = A\, e^{in\alpha}$ (n integer),

$$U_n(r, \vartheta, z) = A\, J_n(\beta r)\, e^{in\vartheta}\, e^{ik\cos\varphi\, z} \qquad (\beta = k \sin\varphi)$$

$$= n\text{th-order Bessel beams}$$

- All of them (except for $n = 0$) have a null on the z-axis
- They present a vortex of charge n at the origin ($r = 0$)
- Any combination of U_n is a diffraction-free beam

Application fields for nondiffracting light beams are virtually infinite (communications, energy concentration, metrology, laser machining, triangulation systems, atom trapping, ...)

The only drawback is that nondiffracting beams are not physically realizable, because they carry an infinite energy:

$$\int I(r) r \, \mathrm{d}r = \infty$$

Nonetheless, approximate versions of nondiffracting beams can be realized. They are generally referred to as *quasi-nondiffracting*, or *pseudo-nondiffracting*, or *limited-diffraction* beams.

A possible experimental set-up

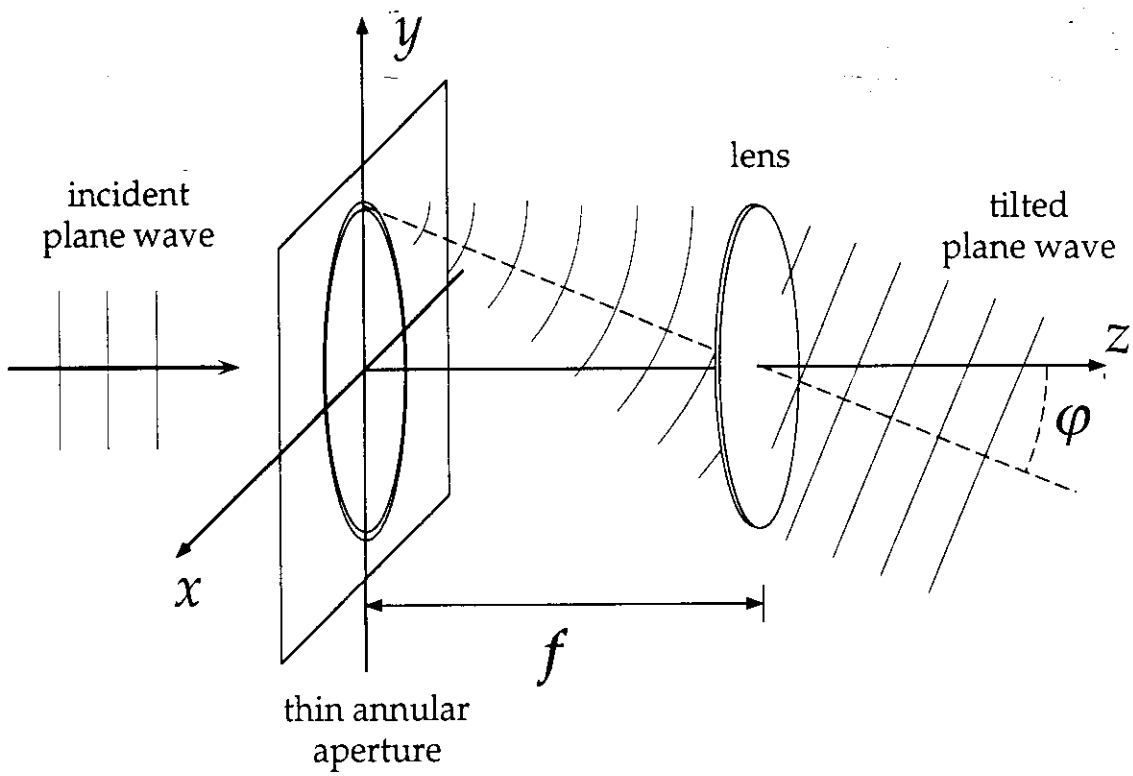

The obtained beam is only approximately nondiffracting, because it maintains its transverse profile up to a finite distance $z_{\max}$ from the lens (*diffraction-free range*).

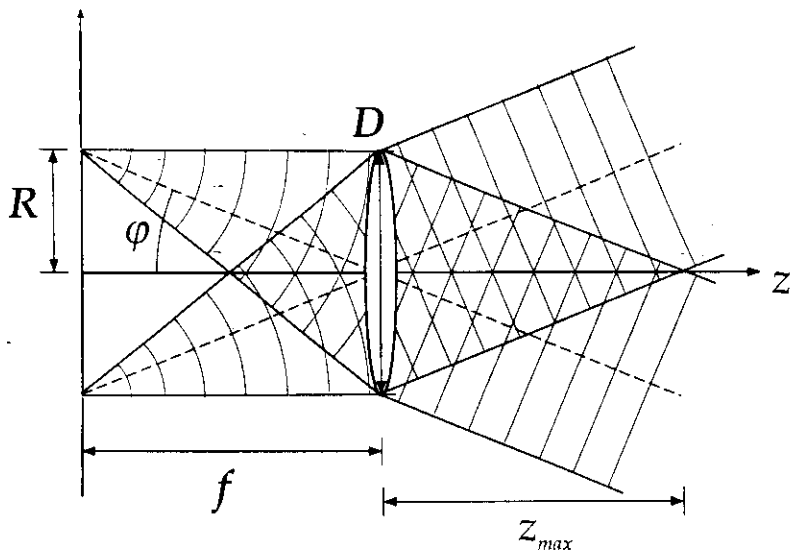

This occurs because the plane waves are truncated by the lens, and truncated "plane waves" overlap only within a finite distance.

$$\varphi \approx \frac{R}{f}\,; \qquad z_{max} \approx \frac{D}{2\varphi}$$

Any transverse limitation of the beam leads to a reduction of the diffraction-free range

Apertured Bessel beams

All we can physically obtain is an apertured version of a Bessel beam, so that:

$$U(r, \vartheta, 0) = AJ_n(\beta r)e^{in\vartheta} f(r)$$

The presence of the windowing function $f(r)$ generally gives rise to complicated expressions for the propagated beam.

The shape of the windowing function influences the features of the beams on propagation.

Which choice for $f(r)$?

- circ function (as in the previuos set-up)

$$f(r) = \text{circ}\left(\frac{2r}{D}\right)$$

It is the most natural choice, but presents some drawbacks related to the oscillating behavior of the on-axis intensity, to be ascribed to the Fresnel diffraction of the component plane waves by the circular aperture.

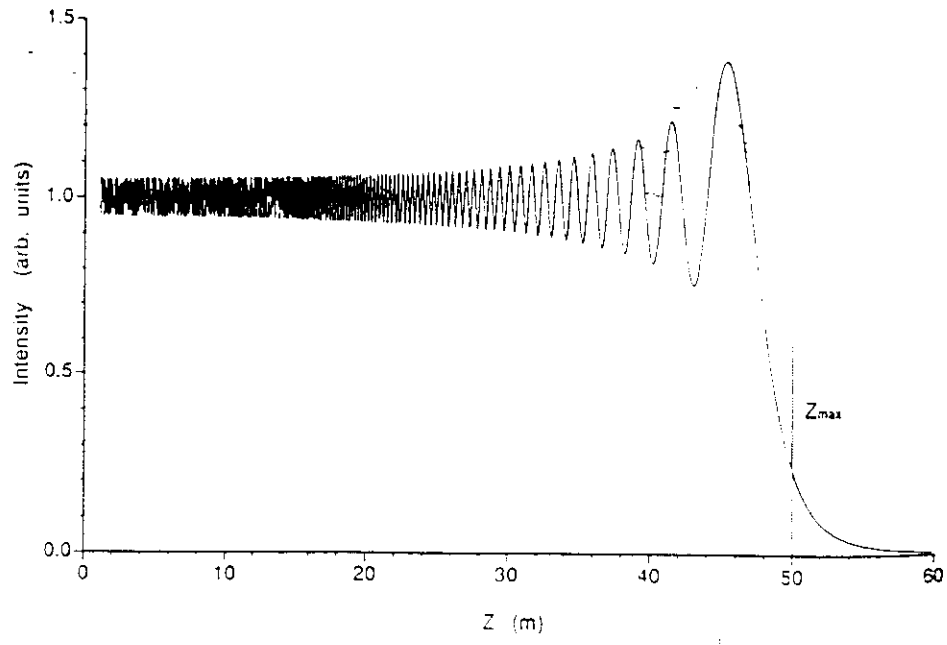

- Gaussian function

$$f(r) = \exp\left(-\frac{r^2}{w_0^2}\right)$$

It gives rise to the *Bessel–Gauss beams* (BGB).

They are the most widely known and studied quasi-nondiffracting beams, because of their very appealing analytical features.

Within the paraxial approximation:

$$\begin{aligned} U_n(r,\theta,z) &= A\left(\frac{w_0^2}{w_c^2}\right) J_n\left(\frac{w_0^2}{w_c^2}\beta r\right) \\ &\quad \times \exp\left[-\frac{r^2+z^2\beta^2/k^2}{w_c^2}\right] \exp(in\theta) \end{aligned}$$

where $w_c^2 = w_0^2 + 2iz/k$

on-axis intensity ($L = kw_0^2/2$)

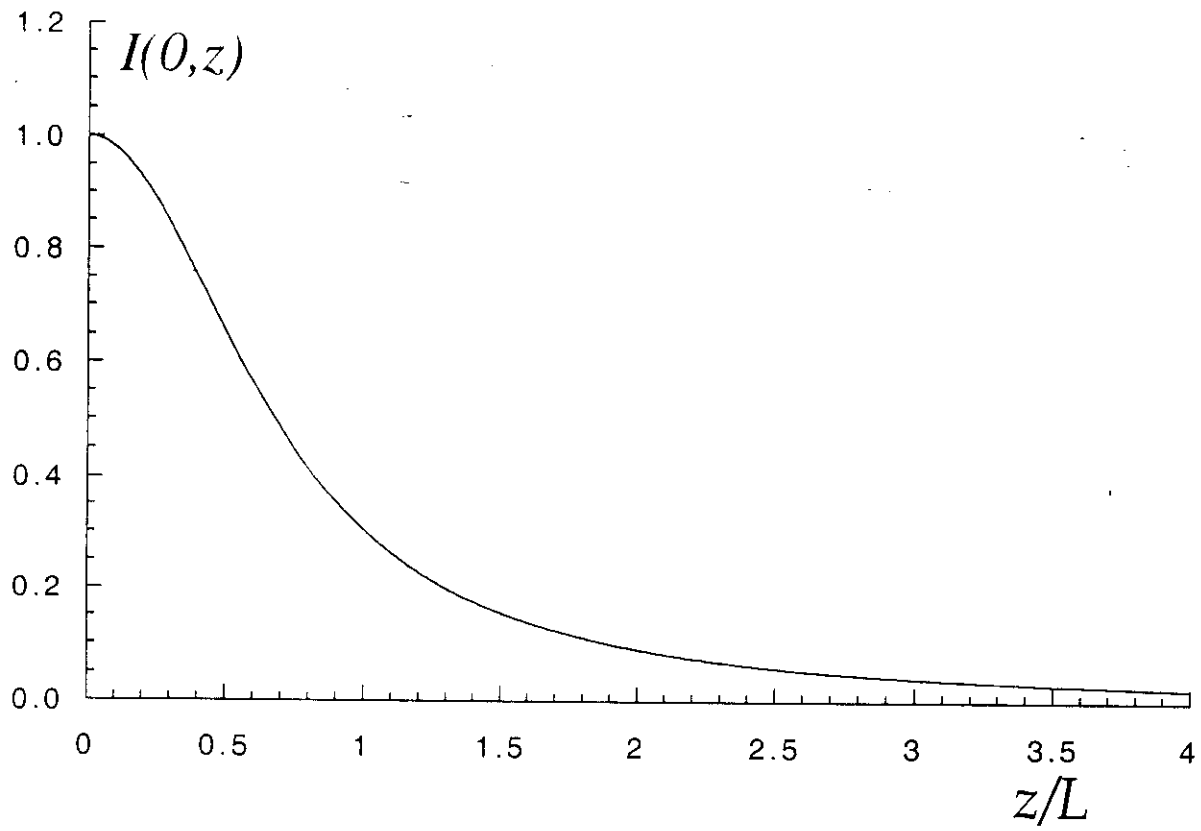

They can be viewed as the superposition of fundamental Gaussian beams on a cone:

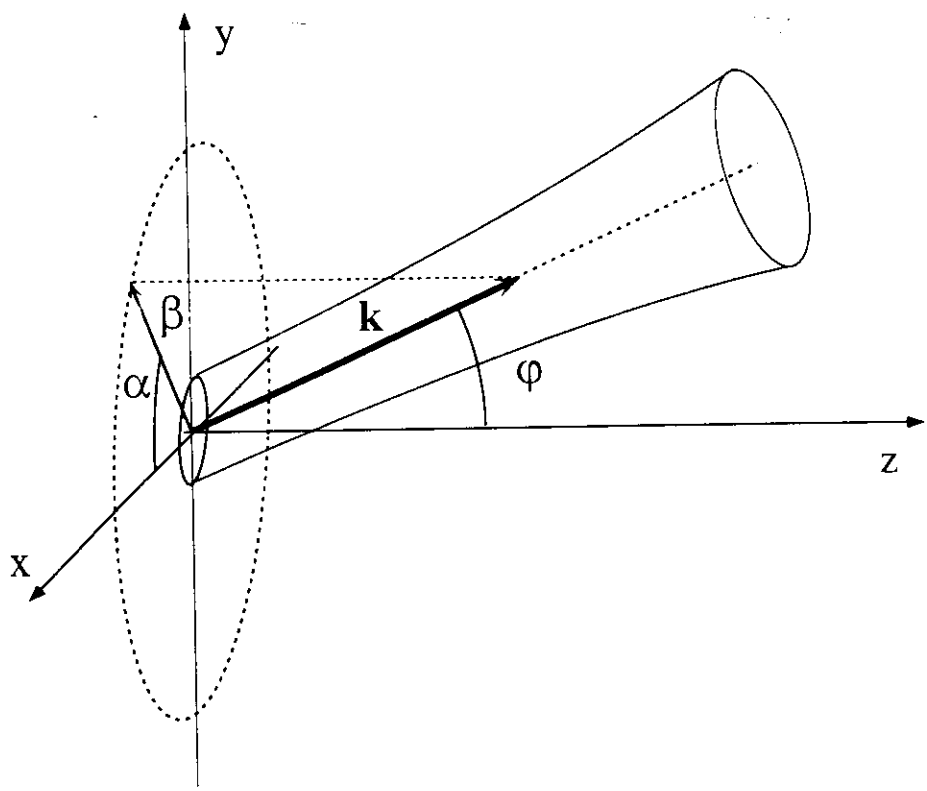

The diffraction-free range can be expressed in terms of the spot size w_0 and the cone angle φ:

$$z_{\max} \approx \frac{w_0}{\tan \phi}$$

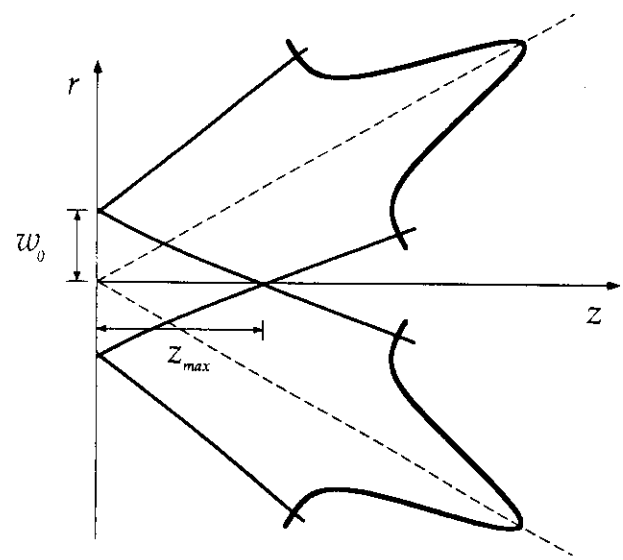

For $z > z_{\max}$ the transverse profile tends to a Gaussianly-shaped annulus.

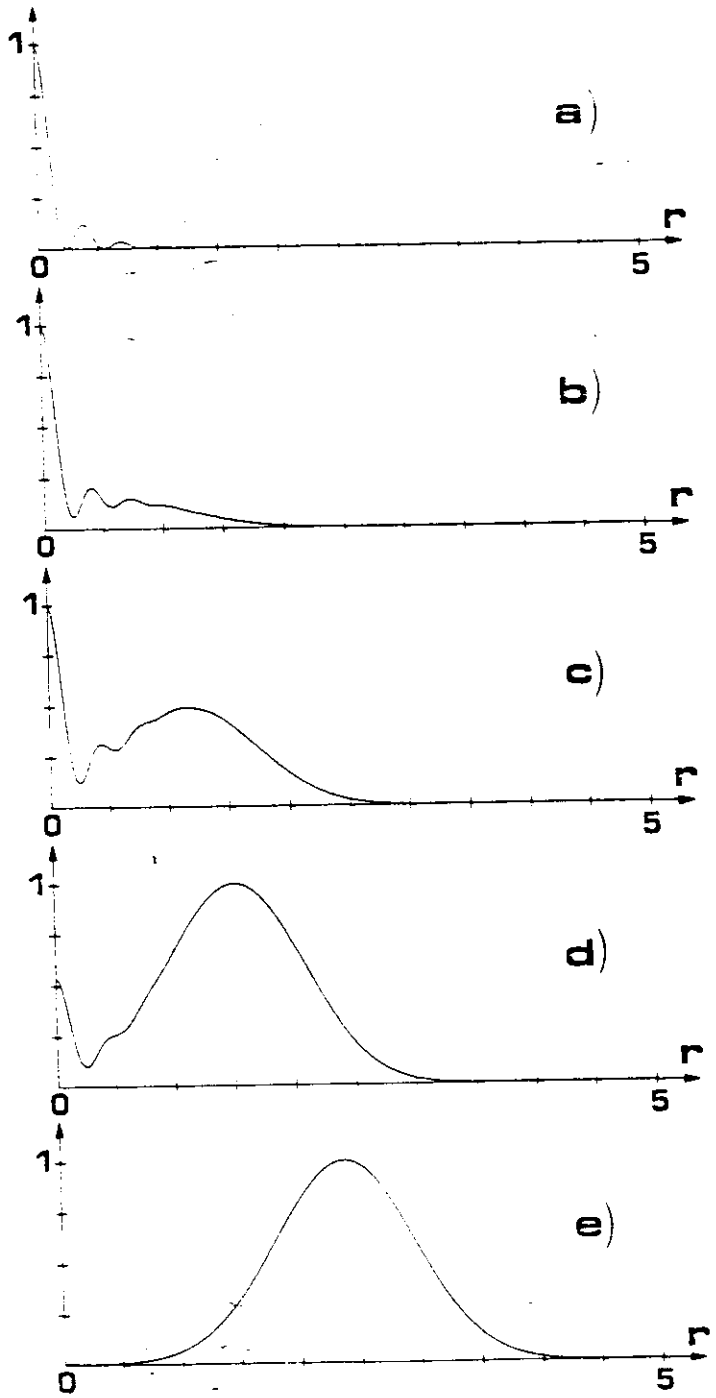
1
a)
r
0
5
1
b)
r
0
5
1
c)
r
0
5
1
d)
r
0
5
1
e)
r
0
5

- Flat-top windowing profile (a good compromise):

  $f(r) = \mathrm{SG}_\gamma(r, v_0)$ (Super-Gaussian)

  or

  $f(r) = \mathrm{FG}_N(r, v_0)$ (Flattened-Gaussian)

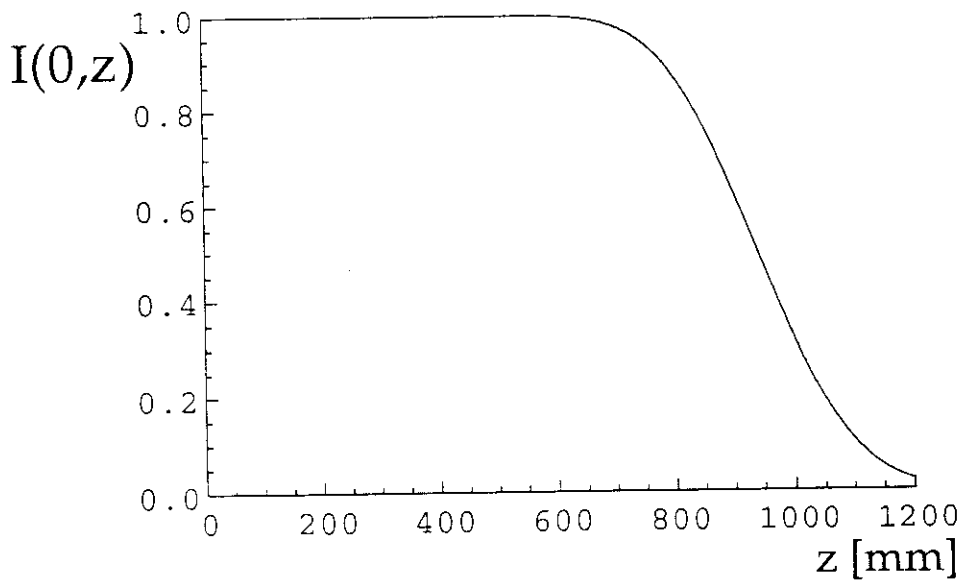

The resemblance effect

The on-axis profile of an apertured Bessel beam seems to reproduce, in some way, the shape of the aperturing function.

This fact can be understood by recalling the superposition scheme in terms of plane waves on a cone.

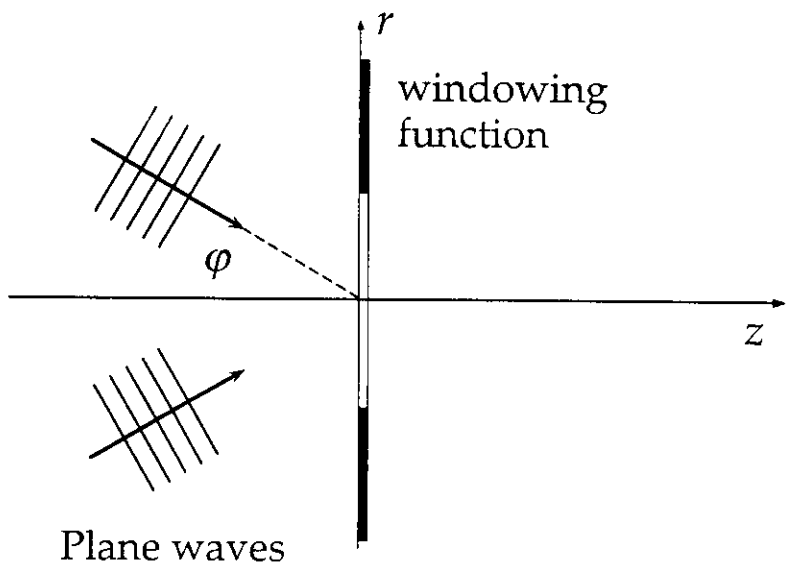

Each plane wave is diffracted by the aperture

All the plane waves on the cone produce the same on-axis field

Within the paraxial approximation, the following schemes are equivalent:

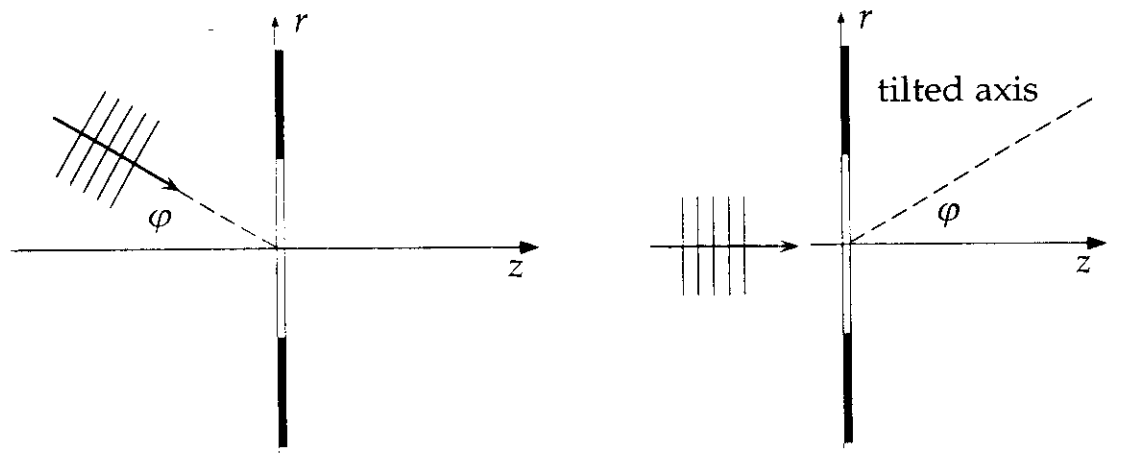

(a) (b)

$\Rightarrow$ the on-axis field in Fig. (a) corresponds to the field in Fig. (b), say V, evaluated along the tilted axis ($r = z \sin\varphi$).

In formulas, we have:

$$|U(0,z)|^2 = |V(z\sin\varphi, z)|^2$$

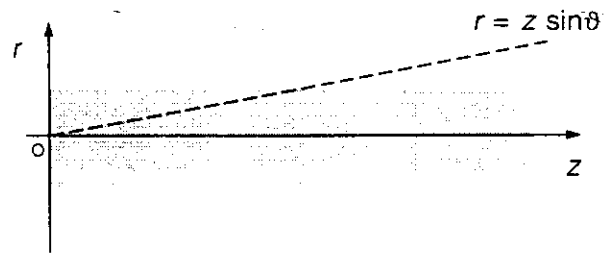

(a)

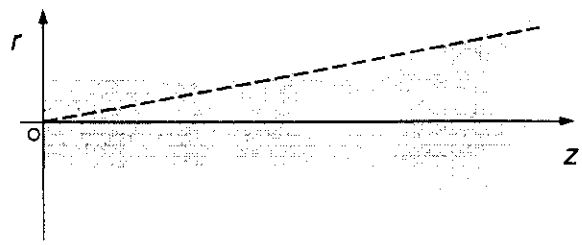

(b)

On-axis intensities for a flattened aperturing function for different values of the steepness (FG profile with different N-values)

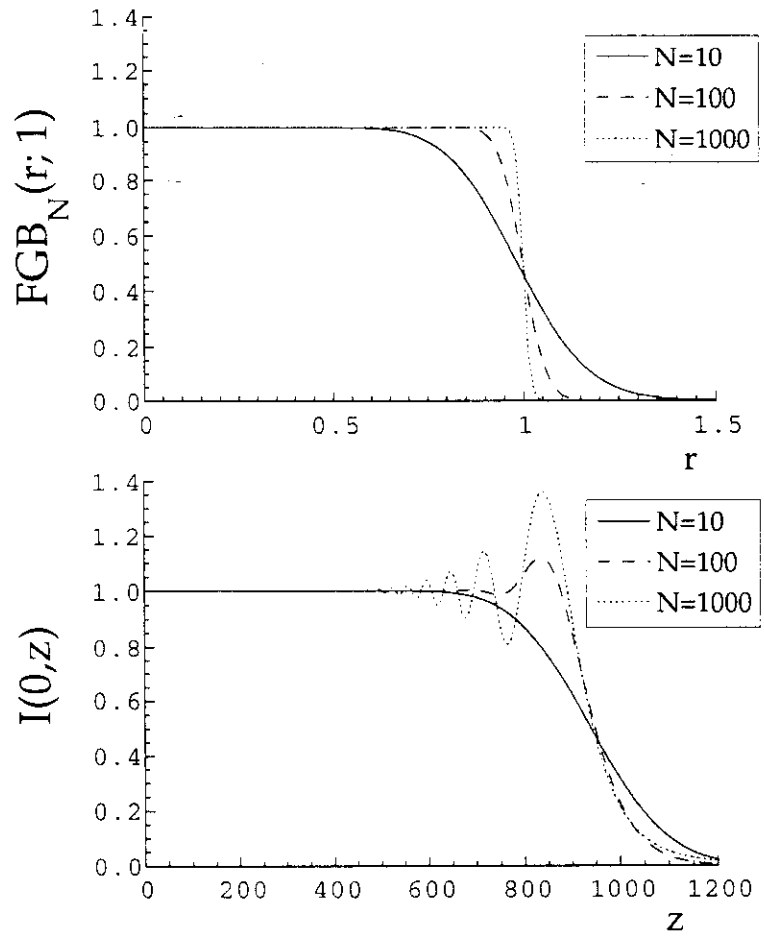

Second-order moments

Is the behavior of nondiffracting, or quasi-nondiffracting beams compatible with the general laws of the moment propagation?

- Moments of Bessel beams cannot be calculated because of their infinite energy.

- Moments of apertured Bessel beams, in some cases, can.

- The behavior of the moments of a Bessel beam can be obtained through a limiting procedure (aperture size $\rightarrow \infty$).

The case of a Bessel–Gauss beam of zero order:

on incresing the spot size of the Gaussian windowing function (keeping fixed the size of the central lobe of the beam) it becomes more and more similar to a Bessel beam.

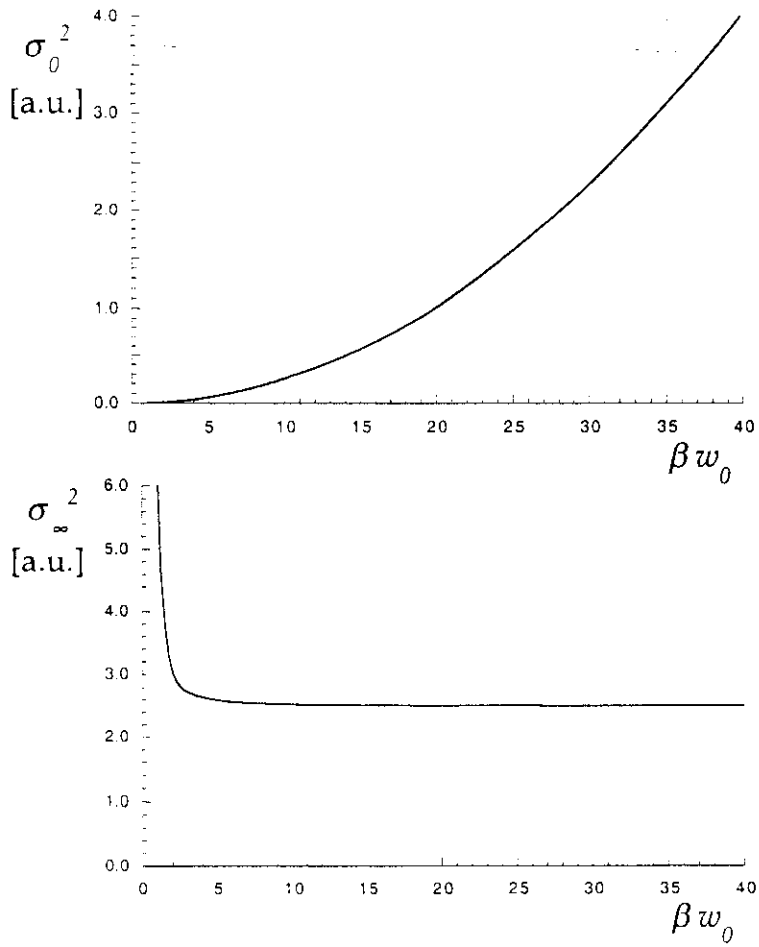

The M^2 factor can be evaluated:

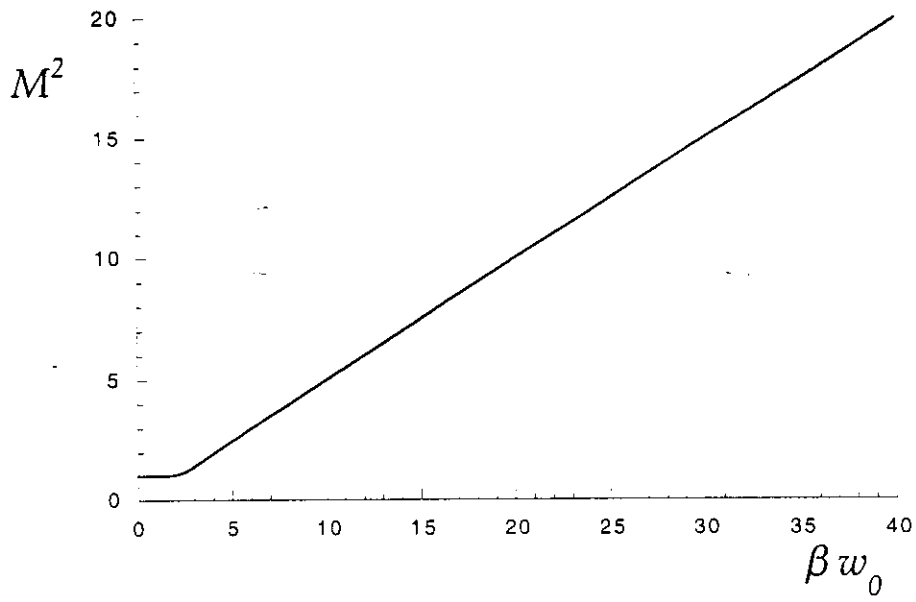

The propagation laws of the second-order moments are still valid, but they do not give useful information about the nondiffracting properties of the beam.

M^2 diverges in the limit of a pure Bessel beam.

If $w_0 \ll 1/\beta$ the BGB tends to a fundamental Gaussian beam, so that $M^2 = 1$.

Generation of quasi-nondiffracting beams through optical elements

- Refractive Optical Elements:

  The superposition scheme in the two-dimensional case can be realized by means of a prism:

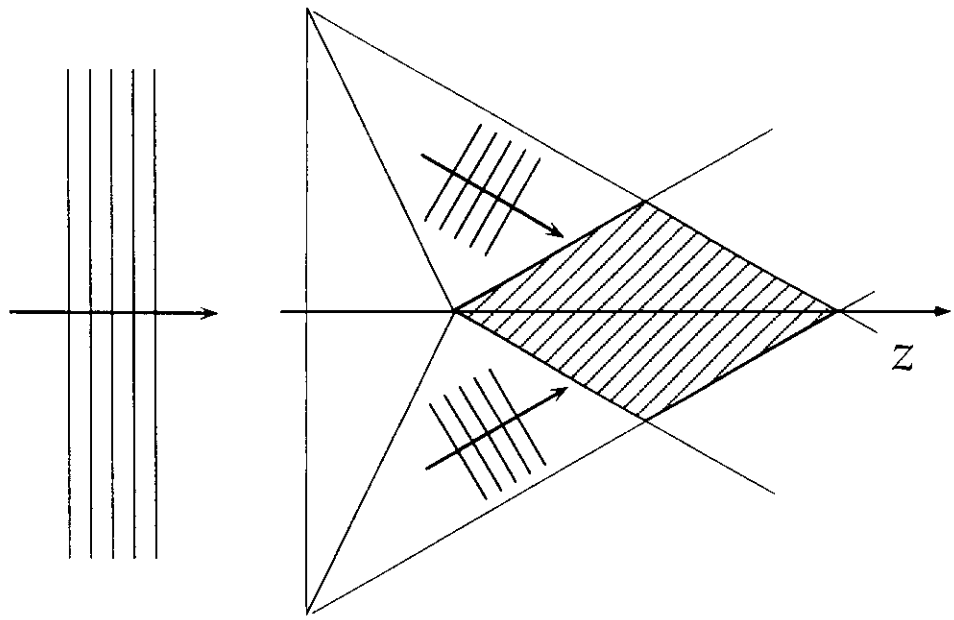

triangular prism

In three dimensions:

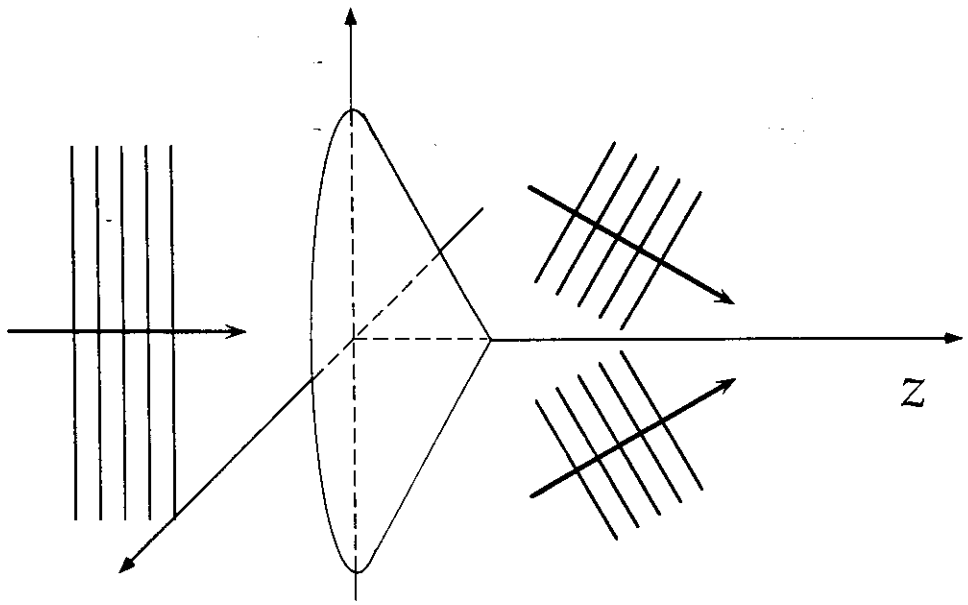

axicon

The rotationally symmetric threedimensional version of a prism is an *axicon*.

Some features:

- The ouput beam can be well *approximated* by a (truncated) Bessel beam.

- The on-axis intensity is expected to increase with the distance from the element, up to a maximum value, and then to decrease.

- Higher-order Bessel beams could be obtained through a modified axicon (*trochoson*), which introduces a vortex in the phase profile of the beam.

- Refractive optical elements are not very convenient for generating non-diffracting beams.

- Diffractive Optical Elements:

  The axicon gives the incident field a phase structure of the type:

  $$e^{-i\beta r},$$

  which corresponds to the transmission function of a "radial" prism.

  The same function as an axicon can be performed by a DOE (*Diffractive Optical Element*):

  - DOE's exploit diffraction (instead of refraction, as conventional optical elements do) to perform unconventional transformations of a beam.

  - Phase-only DOE's generally consist in microstructures engraved on a dielectric substrate, and give rise to the maximum diffraction efficiency.

  - They are much lighter, cheaper, and more versatile than refractive optical elements

    $\rightarrow$ synthesis of *generalized* axicons

References

[1] McLeod, "The axicon: a new type of optical element," Journal of Optical Society of America **44**, 592 (1954).

[2] Durnin et al., "Diffraction-free beams," Physical Review Letters **58**, 1499 (1987).

[3] Durnin, "Exact solutions for nondiffracting beams. I. The scalar theory," Journal of Optical Society of America A **4**, 651 (1987).

[4] Gori et al., "Bessel-Gauss beams," Optics Communications **64**, 491 (1987).

[5] Turunen et al., "Holographic generation of diffraction-free beams," Applied Optics **27**, 3959 (1988).

[6] Durnin et al., Comparison of Bessel and Gaussian beams Optics Letters **13**, 79 (1988).

[7] Wolf, "Diffraction-free beams remain diffraction free under all paraxial optical transformations," Physical Review Letters **60**, 757 (1988).

[8] Indebetouw, "Nondiffracting optical fields: some remarks on their analysis and synthesis," Journal of Optical Society of America A**6**, 150 (1989).

[9] Zahid et al., "Directionality of partially coherent Bessel-Gauss beams," Optics Communications **70**, 361 (1989).

[10] Vasara et al., "Realization of general nondiffracting beams with computer-generated holograms," Journal of Optical Society of America A **6**, 1748 (1989).

[11] Bloisi et al., "Comparison of nondiffracting laser beams," Optics Communications **75**, 353 (1990).

[12] Romea et al., "Modeling of inverse Cerenkov laser acceleration with axicon laser-beam focusing," Physical Review D **42**, 1807 (1990).

[13] De Nicola, "Irradiance from an aperture with a truncated J_0 Bessel beam," Optics Communications **80**, 299 (1991).

[14] Overfelt et al., "Comparison of the propagating characteristics of Bessel, Bessel-Gauss, and Gaussian beams diffracted by a circular aperture," Journal of Optical Society of America A **8**, 732 (1991).

[15] Mishra, "A vector wave analysis of a Bessel beam," Optics Communications **85**, 159 (1991).

[16] Cox et al., "Holographic reproduction of a diffraction-free beam," Applied Optics **30**, 1330 (1991).

[17] Cox et al., "Nondiffracting beam from a spatially filtered Fabry-Perot resonator," Journal of Optical Society of America A **9**, 282 (1992).

[18] Lin et al., "Experimental investigation of Bessel beam characteristics," Applied Optics **31**, 2708 (1992).

[19] Staronski et al., "Lateral distribution and flow of energy in uniform-intensity axicons," Journal of Optical Society of America A **9**, 2091 (1992).

[20] Cox et al., "Constant-axial-intensity nondiffracting beam," Optics Letters **17**, 232 (1992).

[21] Sochacki et al., "Nonparaxial design of generalized axicons," Applied Optics **31**, 5326 (1992).

[22] Davidson et al., "Efficient formation of nondiffracting beams with uniform intensity along the propagation direction," Optics Communications **88**, 326 (1992).

[23] Iftekharuddin, "Heterodyne detection by using a diffraction-free beam: tilt and offset effects," Applied Optics **31**, 4853 (1992).

[24] Jaroszewics et al., "Apodized annular-aperture-logarithmic axicon: smoothness and uniformity of intensity distributions," Optics Letters **18**, 1893 (1993).

[25] Davis et al., "Diffraction-free beams generated with programmable spatial light modulators," Applied Optics **32**, 6368 (1993).

[26] Iftekharuddin et al., "Heterodyne detection using a diffraction-free beam: background-noise effects," Applied Optics **32**, 3144 (1993).

[27] Piquero et al., "Quality changes of gaussian beams propagating through axicons," Optics Communications **105**, 289 (1994).

[28] Lohmann et al., "Bessel functions: parallel display and processing," Optics Letters **19**, 55 (1994).

[29] Lü et al., "Focal shift in unapertured Bessel-Gauss beams," Optics Communications **109**, 43 (1994).

[30] Rosen, "Synthesis of nondiffracting beams in free space," Optics Letters **19**, 369 (1994).

[31] Jordan et al., "Free-space azimuthal paraxial wave equation: the azimuthal Bessel-Gauss beam solution," Optics Letters **19**, 427 (1994).

[32] Kowarz et al., "Bessel-beam representation for partially coherent fields," Journal of Optical Society of America A **12**, 1324 (1995).

[33] Bouchal et al., "Non-diffractive vector Bessel beams," Journal of Modern Optics **42**, 1555 (1995).

[34] Popov et al., "Linear axicons in partially coherent light," Optical Engineering **34**, 2567 (1995).

[35] Klewitz et al., "Bessel-beam-pumped tunable distributed-feedback laser," Applied Optics **34**, 7670 (1995).

[36] Lü et al., "Three-dimensional intensity distribution of focused Bessel-Gauss beams," Journal of Modern Optics **43**, 509 (1996).

[37] Chávez-Cherda et al., "Nondiffracting beams: travelling, standing, rotating and spiral waves" Optics Communications **123**, 225 (1996).

[38] Paterson et al., "High-order Bessel waves produced by axicon-type computer-generated holograms," Optics Communications **124**, 121 (1996).

[39] MacDonald, "Interboard optical data distribution by Bessel beam shadowing," Optics Communications **122**, 169 (1996).

[40] Zhao et al., "Comparison of transformation characteristics of linearly polarized and azimuthally polarized Bessel-Gauss beams," Optics Communications **131**, 8 (1996).

[41] Kotlyar et al., "Calculation of phase formers of non-diffracting images and a set of concentric rings," Optik **102**, 45 (1996).

[42] Jaroszewicz et al., "Diffractive patterns of small cores generated by interference of Bessel beams," Optics Letters **21**, 839 (1996).

[43] Bagini et al., "Generalized Bessel-Gauss beams," Journal of Modern Optics **43**, 1155 (1996).

[44] Palma et al., "Imaging of generalkized Bessel-Gauss beams," Journal of Modern Optics **43**, 2269 (1996).

[45] Santarsiero, "Propagation of generalized Bessel-Gauss beam through ABCD optical systems," Optics Communications **132**, 1 (1996).

[46] De Nicola, "On-axis focal shift-effects in focused truncated J_0 Bessel beams," Pure and Applied Optics **5**, 827 (1996).

[47] Piskerskas et al., "Optical parametric oscillator pumped by a Bessel beam," Applied Optics **36**, 7779 (1997).

[48] Liu et al., "Effects of different apertured modulations on propagation features of the first-order Bessel beam," Optik **106**, 53 (1997).

[49] Borghi et al., "Axial intensity of apertured Bessel beams," Journal of Optical Society of America A **14**, 23 (1997).

[50] Borghi et al., "M^2 factor of Bessel-Gauss beams," Optics Letters **22**, 262 (1997).

[51] Horák et al., "Nondiffracting stationary electromagnetic field," Optics Communications **133**, 315 (1997).

[52] Overfelt, "Generation of a Bessel-Gauss pulse from a moving disk source distribution," Journal of Optical Society of America A **14**, 1087 (1997).

[53] Arif et al., "Two-element refracting system for annular Gaussian-to-Bessel beam transformation," Applied Optics **37**, 4206 (1998).

[54] Cong et al., "Generation of nondiffracting beams by diffractive phase elements," Journal of Optical Society of America A **15**, 2362 (1998).

[55] Liu et al., "Generation of pseudo-nondiffracting beams with use of diffractive phase elements designed by the conjugate-gradient method," Journal of Optical Society of America A **15**, 144 (1998).

[56] Ding et al., "Approximate description for Bessel, Bessel-Gauss, and Gaussian beams with finite aperture," Journal of Optical Society of America A **16**, 1286 (1999).

[57] Guérineau et al., "Nondiffracting array generation using an N-wave interferometer," Journal of Optical Society of America A **16**, 293 (1999).

[58] Zhang et al., "Coherent-mode decomposition of Bessel-Gauss beams," Journal of Optical Society of America A **16**, 1413 (1999).

[59] Jaroszewicz et al., "Lens axicons: systems composed of a diverging aberrated lens and a converging aberrated lens," Journal of Optical Society of America A **16**, 191 (1999).